Parameterization of the Urban Water Budget with the Submesoscale Soil Model

SYLVAIN DUPONT, PATRICE G. MESTAYER, AND EMMANUEL GUILLOTEAU

Laboratoire de Mécanique des Fluides, Ecole Centrale de Nantes, Nantes, France

EMMANUEL BERTHIER AND HERVÉ ANDRIEU

Laboratoire Central des Ponts et Chaussées, Nantes, France

(Manuscript received 23 February 2005, in final form 25 August 2005)

ABSTRACT

This paper presents the hydrological component of the Submesoscale Soil Model, urbanized version (SM2-U). This model is an extension of the rural Interactions between Soil, Biosphere, and Atmosphere (ISBA) soil model to urban surfaces. It considers in detail both rural and urban surfaces. Its purpose is to compute the sensible heat and humidity fluxes at the canopy–atmosphere interface for the computational domain lower boundary condition of atmospheric mesoscale models in order to simulate the urban boundary layer in any weather conditions. Because it computes separately the surface temperature of each land use cover mode while the original model computes a unique temperature for the soil and vegetation system, the new version is first validated for rural grounds by comparison with experimental data from the Hydrological Atmospheric Pilot Experiment-Modélisation du Bilan Hydrique (HAPEX-MOBILHY) and the European Field Experiment in a Desertification Threatened Area (EFEDA). The SM2-U water budget is then evaluated on the experimental data obtained at a suburban site in the Nantes urban area (Rezé, France), both on an annual scale and for two stormy events. SM2-U evaluates correctly the water flow measured in the drainage network (DN) at the annual scale and for the summer storm. As for the winter storm, when the soil is saturated, the simulation shows that water infiltration from the soil to the DN must be taken care of to evaluate correctly the DN flow. Yet, the addition of this soil water infiltration to the DN does not make any difference in the simulated surface fluxes that are the model outputs for simulating the urban boundary layer. Urban hydrological parameters are shown to largely influence the available water on artificial surfaces for evaporation and to influence less the evapotranspiration from natural surfaces. The influence of the water budget and surface structure on the suburban site local climatology is demonstrated.

1. Introduction

The accurate simulation of the atmospheric boundary layer over urban areas with mesoscale models requires a detailed representation of the sensible and latent heat fluxes at the canopy–atmosphere interface. This may be obtained by a soil model that takes into account the specific features of the urban surface covers and the presence of the buildings forming a urban canopy with specific processes such as radiation trapping, building wall heat transfers and storage, anthropogenic heat sources, and precipitation water provisional storage, runoff, and drain away. While the traditional approach in mesoscale models was to represent urban areas analogous to soil surfaces, several models/schemes have been recently developed that may improve the urban canopy parameterization in simulations of the urban climatology, urban heat island, and, indirectly, urban air quality. Best (2005) developed a simple urban parameterization for operational numerical weather prediction models at a horizontal resolution of about 12 km, where urban areas are represented as a canopy of concrete. The local-scale urban meteorological parameterization scheme (LUMPS) model of Grimmond and Oke (2002) computes the energy budget by means of some semiempirical parameterizations based on measurements over a dozen American cities, especially the objective hysteresis model (OHM; Grimmond and Oke 1999) based on empirical correlation between the heat storage in the urban fabric, net radiation, and

Corresponding author address: Sylvain Dupont, EPHYSE, INRA Bordeaux, BP 81, F-33883 Villenave d'Ornon, France.
E-mail: sdupont@bordeaux.inra.fr

urban land cover fractions. The single-layer urban canopy model of Masson (2000) and the multilayer urban canopy model of Martilli et al. (2002) compute explicitly the heat and radiation transfers of all street surfaces (roofs, walls, and pavements) while reducing the urban canopy to a regular array of identical streets, with Masson (2000) assuming equiprobable directions (isotropy assumption) and Martilli et al. (2002) a unique street direction. These last two models are exclusively urban, ignoring small and large vegetated areas as well as empty areas; for simulations of large areas they must therefore be associated with a rural soil model that represents the transfers at natural surfaces. A tiling approach may be used to represent the heterogeneity of real urban areas (Lemonsu and Masson 2002), but with the disadvantage that the two schemes (urban and rural) are separated, thus truncating the heat and water exchanges at the subgrid scale. Using two incompatible schemes for representing the city grounds—an urban one for the "paved city" and a rural one for the "vegetated city"—does not seem a good approach, especially for studying the urban microclimatology. It emphasizes the vertical transfers and skips the interactions between the different cover modes, such as surface water runoff from the artificial surfaces, horizontal water transfers under the neighboring surfaces, and dispersed vegetation interspersed between buildings or in streets and squares.

For their implementation with operational forecasts these models must work under all meteorological conditions, while they have been validated for clear-sky conditions when the urban thermal influence is largest, which are also favorable conditions for both the urban heat island development and the air quality deterioration. Yet, the water budget calculation is an important component of these models because it is interlinked with the thermal component through evaporation and because the latent heat flux has a potentially large influence on the atmospheric thermal stratification. This flux depends on the land use and is highly variable, especially in urbanized areas; it may be large for some areas where the vegetation cover fraction is large, especially with irrigation, while over artificial surfaces it is usually small but increases dramatically when the surfaces are wet immediately after rain events. Also, the presence of water surfaces interspersed among dry surfaces enhances their evaporation. A larger part of the water falling on urban surfaces is collected and transferred to the drainage network (DN), removing from the surface or from the superficial soil some water that would otherwise be available for evapotranspiration.

Urban hydrologists have focused on the simulation of flow during rain events, which are necessary for designing the sewer network and reducing the pollution conveyed in rainwater runoff. This explains why the flow rate into the network is often the only variable that is well documented experimentally. Because there are nearly no urban evaporation datasets available for long periods, validation of the water flow to the DN appears as a first step in evaluating the computation of the water budget and evapotranspiration in urban areas. Different urban water budget schemes have been developed based on different concepts and with different levels of complexity depending on the intended application. The complexity level of these models is generally proportional to the number of soil layers. Several models are in operational use today to simulate the flow rate of an urban catchment during storm events, for example, the Storm Water Management Model (SWMM; Rossman 2004), the integrated modeling package for urban drainage and sewer systems (MOUSE; Danish Hydraulic Institute 1996), "HydroWorks" (Wallingford Software, Ltd. 1997), and "CANOE" (INSAVALOR and Sogreah 1997). These models consider precipitation as input and simulate the surface runoff and infiltration as well as groundwater transfers to the drainage network and water flow in drainage sewer systems. At a finer scale and for research purpose, the Urban Hydrological Element (UHE) model has been developed by Berthier et al. (2004) with the purpose of accounting the role of the soil on the generation of urban flow rates. Soil water flows are solved with a finite-element code on a two-dimensional vertical domain representing a cross section of a typical urban parcel. UHE simplifies the atmospheric processes but details the water runoff flows over natural and (semi) impervious surfaces and the transfers within the soil (using a finite-element calculation method), with a special focus on the influence of the water infiltration from the soil to the DN because of its water-tightness defects. Belhadj et al. (1995) showed that a sewer system, although not intended to receive rainwater, does respond to rainfall when the saturation level reaches the depth of the network—the pipes are not watertight and the sewer system acts as a drain. Grimmond and Oke (1991) developed a one-layer urban canopy model with zero soil layer, which allows for an estimation of the hourly and longer-period urban evapotranspiration. Also, Jia et al.'s (2001) Water and Energy Transfer Processes (WEP) multilayer model simulates the water and energy transfers that are spatially distributed in rural and urban watersheds by computing the land surface temperature and evapotranspiration.

The Submesoscale Soil Model, urbanized version, (SM2-U) has been developed for providing the input data at the lower boundary of atmospheric mesoscale

models for simulations at very fine spatial resolution (less than a kilometer) (Guilloteau 1999; Dupont 2001). It is used for studies of urban micrometeorology and microclimatology as well as for high-resolution air quality simulations (Dupont et al. 2004a). It has been implemented with numerical weather prediction models such as the fifth-generation Pennsylvania State University (PSU)–National Center for Atmospheric Research (NCAR) Mesoscale Model (MM5; Dupont et al. 2004a), the Advanced Regional Prediction System (ARPS; Dupont and Mestayer 2006), and the High Resolution Limited Area Model (HIRLAM; Mahura et al. 2004). Starting from Pleim and Xiu's (1995) version of the "force–restore" rural soil model of Noilhan and Planton (1989), later known as the Interaction between the Soil–Biosphere–Atmosphere (ISBA; see Noilhan and Mahfouf 1996), SM2-U was developed on physical bases to extend ISBA by including the urban surfaces such as road systems, housings in low and high densities, and dense continuous urban canopies. SM2-U has thus the advantage to model in a unique code all of the soils encountered in an urban area from the rural outskirts to the city centers, with any distribution of surface cover fractions, keeping all of the schemes for the natural soils with vegetation that were extensively validated in the various comparisons of ISBA with experimental data (e.g., Giordani et al. 1996). SM2-U includes a one-layer urban-and-vegetation canopy model to integrate the physical processes inside the urban canopy and three soil layers as introduced by Boone et al. (1999) in the latest version of ISBA.

This article focuses on the SM2-U hydrological component. Its thermal component is described and tested elsewhere (Dupont et al. 2002; Dupont and Mestayer 2004, 2006) and is only very briefly sketched here. The general principles and the water budget equations are described in section 2.

As compared with ISBA, which computes the budgets for the whole ground and vegetation system with one composite surface temperature per cell, the approach of SM2-U consists of separating the budgets for each cover mode, using the same equations as in the original model with only a few constant readjustments. It was therefore needed at first to check how much this difference influences the simulation of rural grounds. Thus, SM2-U is first validated with the Hydrological Atmospheric Pilot Experiment-Modélisation du Bilan Hydrique (HAPEX-MOBILHY) and European Field Experiment in a Desertification Threatened Area (EFEDA) experimental campaigns that have been extensively studied with various versions of ISBA (see, e.g., Shao and Henderson-Sellers 1996; Boone et al. 1999) and with the preurban version of SM2-U, called SM2-ISBA (for the small differences between ISBA and SM2-ISBA, mostly in numerical methods, and for their performances, see Guilbaud 1996). Data from the HAPEX-MOBILHY allow model validation over a full year, that is, for various seasonal variations, while the EFEDA concerns a short period in a semiarid area allowing a test with a good quality model initialization.

Then, the model is compared with the experimental data obtained on a small suburban catchment of Rezé (France) (Berthier et al. 1999). SM2-U flow discharge to the DN is compared with the water flow measured at the DN outlet. In addition, SM2-U simulations are compared with results obtained with the UHE model (Berthier et al. 2004). The comparison with this hydrological model is of double interest for (i) a better evaluation of SM2-U accuracy and (ii) an analysis of SM2-U realism against a physically based hydrological model, both of which may prove helpful to improve SM2-U. A simulation is presented where the water infiltration from the soil to the DN is added to the model to evaluate this process's influence on the water budget and surface evaporation. Then, a preliminary sensitivity study of the model results to the hydrological parameters of the artificial surfaces is reported, followed by a simulation exercise demonstrating the influence of the local water budget and the surface cover management on the local climatology.

2. Model description

a. General presentation

SM2-U is an extension of the force-restore model of Noilhan and Planton (1989) that keeps its principal characteristics, equations, and coefficients, and only the changes to the original model are detailed here. While ISBA computes the budgets for the whole ground–vegetation system for a natural soil partly covered with vegetation, in each computational cell SM2-U accounts for the following eight surface types (Fig. 1): the natural surfaces—bare soil without vegetation "bare," soil located between vegetation elements "nat," and the vegetation cover "vegn"; the artificial surfaces—building roofs "roof," paved surfaces without vegetation "pav," vegetation elements over the paved surface (e.g., roadside trees) "vega," and the paved surface under the vegetation "cova"; and the water surfaces "wat." Each surface type is characterized by its area fraction f_i, with $\Sigma_i\,(f_i) = 1$, for $i \in$ {bare, nat, pav, roof, vega, vegn, wat} in each grid cell and $f_{\text{vega}} = f_{\text{cova}}$.

SM2-U computes the water content in three soil layers. The thin "surface layer" acts as a buffer reservoir for the evaporation from the soil surface and the transfer to/from the second layer. The root-influenced layer

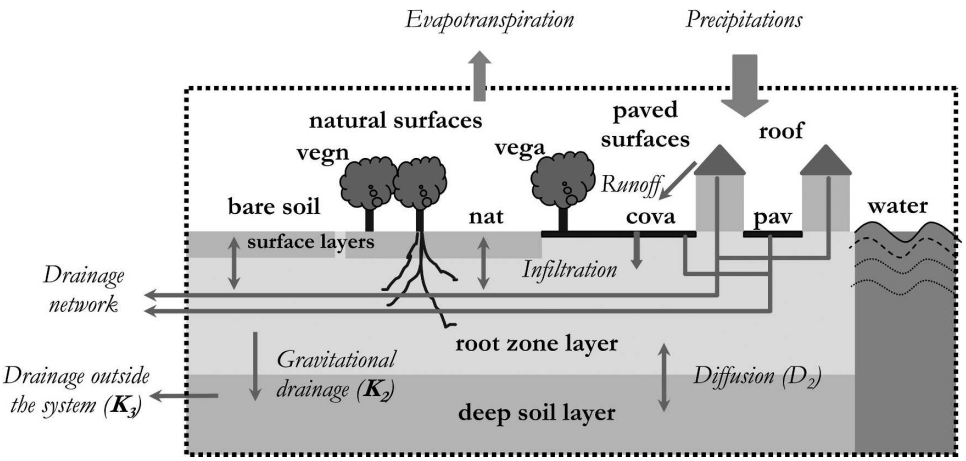

FIG. 1. Scheme of the SM2-U water budget model.

models the water content available for vegetation transpiration. The subroot layer, or "deep soil layer," is used as a water reservoir to provide water to the root zone layer by diffusion in dry periods, as introduced by Boone et al. (1999) in the three-layer ISBA model version (ISBA-3L). For vegetation, roofs, and paved surfaces, an interception reservoir defines the maximum amount of retained liquid water. While roof surfaces are assumed to be fully impervious, paved surfaces are semiimpervious and let water infiltrate downward but not upward.

The energy budget is computed for each surface type in the cell

$$R_{n\,i} + Q_{\text{anth}\,i} = H_{\text{sens}\,i} + \text{LE}_i + G_{s\,i}; \qquad (1)$$

then the cell energy fluxes ϕ_{moy} are obtained by averaging the individual fluxes ϕ, weighted by f_i, $\phi_{\text{moy}} = \Sigma_i f_i \phi_i$, where ϕ represents the net radiation flux R_n, the anthropogenic heat flux Q_{anth}, the sensible heat flux H_{sens}, the latent heat flux LE, or the storage heat flux G_s. Actually, G_s is computed as the residual of (1). The computations of the net radiation and sensible and latent heat fluxes, $R_{n\,i}$, $H_{\text{sens}\,i}$, and LE_i, respectively, are similar to those of the original model for the rural surfaces, with the parameters being adapted to urban surface materials, except that the noniterative scheme of Guilloteau (1998) is used to compute the transfer coefficients with different momentum and heat roughness lengths. Here, Q_{anth} is parameterized as a function of human activity; LE is computed from the air specific humidity gradient between the surface and a reference level in the atmosphere as is done in most atmospheric models, allowing simulation of the surface condensation, whereas in hydrological models such as UHE, SWMM, or WEP it is computed from the Penman and Penman–Monteith equations. Hence, to compute the heat fluxes $H_{\text{sens}\,i}$ and LE_i, SM2-U determines the temperature $T_{s\,i}$ and specific humidity $q_{\text{vs}\,i}$ of each surface type, and one deep soil temperature T_{soil}. The $T_{s\,i}$ (in kelvin) is obtained with the force–restore equation (for $q_{\text{vs}\,i}$ see the next section) for natural surfaces [Eq. (2a)], whereas a simple heat conduction equation in a solid is used for artificial surfaces [Eq. (2b)]. Each artificial surface is composed of two layers: a surface layer that allows the cover mode to respond rapidly to the atmospheric forcing variations, and a second layer that allows the cover mode to store heat;

$$\partial T_{s\,i}/\partial \text{t} = C_{T\,s\,i}\, G_{s\,i} - 2\pi\tau^{-1}(T_{s\,i} - T_{\text{soil}}) \quad \text{for} \quad i \in \{\text{bare, nat, pav, vega, vegn}\} \quad \text{and} \qquad (2a)$$

$$\partial T_{s\,i}/\partial \text{t} = C_{T\,s\,i}\, G_{s\,i} \quad \text{for} \quad i \in \{\text{pav, roof}\}, \qquad (2b)$$

where $C_{T\,s\,i}$ represents the surface resistance to the atmospheric forcing and $\tau = 86\,400$ s (1 day). The computation of the surface temperature of water bodies is separated (Dupont 2001). Because the evaporation flux from the paved surface located under the vegetation is neglected, $T_{s\,\text{cova}}$ is not computed. The cell average surface temperature $T_{s\,\text{moy}}$ is

$$T_{s\,\text{moy}} = \sum_i f_i T_{s\,i}. \qquad (3)$$

The deep soil temperature is given by a return-to-equilibrium equation toward an average temperature of surfaces in contact with the soil. It is assumed that the soil located just below the buildings is at the same temperature as the deep soil,

$$\partial T_{\text{soil}}/\partial t = \tau^{-1}(f_{\text{nat}} T_{s\,\text{nat}} + f_{\text{pav}} T_{d\,\text{pav}} + f_{\text{roof}} T_{s\,\text{roof}} + f_{\text{bare}} T_{s\,\text{bare}} + f_{\text{vegn}} T_{s\,\text{vegn}} + f_{\text{vega}} T_{s\,\text{vega}} - T_{\text{soil}})/(1 - f_{\text{wat}}), \qquad (4)$$

where $T_{d\,\mathrm{pav}}$ is the second-layer temperature of pavement.

The model does not compute any horizontal transfers explicitly. Yet, fast transfers in the soil layers are implicitly assumed because soil temperature and water content are unique in a cell. The only horizontal exchanges inside the urban canopy are the water runoffs from the overflowing reservoirs. The radiation exchange between canopy surfaces is parameterized. The influence of subgrid-scale advection is implicitly modeled by the averaging Eqs. (1) and (3).

To keep the model simple, the energy budget of building walls is not computed explicitly; the influence of canopy thickness appears in the equation of the paved surface temperature by (a) adding the heat stored by building walls to the soil storage flux in Eq. (1), (b) adding the wall resistance to the atmospheric forcing in the surface resistance coefficient $C_{T\,\mathrm{pav}}$, and (c) modeling the radiation trapping with an effective street canyon albedo computed with equations similar to those of Masson (2000) (see Dupont and Mestayer 2006). Thus, the paved surface temperature evaluated by SM2-U corresponds to an effective average temperature of street canyons.

While ISBA determines only one surface temperature for the ground–vegetation system, SM2-U distinguishes the surface temperatures of the vegetation $T_{s\,\mathrm{vegn}}$ and bare soil $T_{s\,\mathrm{nat}}$. This modification has been introduced to allow a parallel representation of the vegetation over paved surfaces, especially in view of alternative microclimatological scenarios; a single temperature for the paved surface and its dispersed vegetation would be an erroneous approach, because of the large differences in their thermal properties. This modification of the model generates computational changes of the mean surface temperature and sensible and latent heat fluxes even for rural areas. The heat flux equations are similar but are separated for the bare soil and vegetation, and the evapotranspiration from each rural surface is computed with its own surface temperature, not the cell-averaged temperature.

b. Hydrological component

Because of their different structures the urban surfaces have different hydrological behaviors that vary according to precipitation intensity and duration, and are still poorly known. The underneath of the urban soil is made heterogeneous by the presence of trenches and artifacts, such as, for example, drainage and sewerpipes, cable routes, subway, and so on, which generate specific water fluxes. This heterogeneity complicates the assessment of the water budget in urban areas (Berthier et al. 2004).

SM2-U extends the water budget calculations of ISBA to urban surfaces and includes some recent developments of Boone et al. (1999). The urban soil is assumed homogeneous in each cell: its water content is provided by summing the contributions of all surface types, thus allowing instantaneous horizontal subgrid subsurface water transfers. Intergrid transfers are not computed but are implicit in the second- and third-layer drainages (K_2 and K_3, respectively). Unlike storm water models, our model does not include horizontal water exchanges at the surface, especially those resulting from ground slope, except for the runoff from one impervious surface to the next. Surface runoff on pervious surfaces is not considered. Artificial surfaces such as building roofs and pavement are totally or partially impervious, allowing for temporary storage of the intercepted precipitated water. Waterproof surfaces (roofs) are either connected to the DN or overflow to the neighboring natural (or paved) surface. Paved surfaces are also (partly) connected to the DN. Unlike the WEP and SWMM models, in SM2-U the paved surfaces let some water directly infiltrate downward as in the UHE model. Indeed, Raimbault (1996) estimated that the annual infiltration through a pavement amounts to some 20%–30% of the total rainfall. Following also Raimbault (1996), the upward water flux by capillarity is neglected here and the soil water content does not influence the water budget of the artificial surfaces. The water flow inside the DN is not explicitly simulated in the model as in storm water models, but the flow at the DN outlet may be model output.

1) Intercepted water storage by (semi) impervious surfaces

Impervious and semiimpervious surfaces (pav, cova, roof, vega, and vegn) are considered as water reservoirs, each with a maximum storage capacity above which water runs off. The water contributions to the reservoirs are precipitation and watering P_i, condensation, and, according to the surface type, water runoff from neighboring surfaces. The water losses are evaporation E_i, infiltration in the soil I_i, and water runoff Ru_i toward the neighboring surface and/or the DN.

Therefore, the reservoir water content budget equation is

$$\partial w_{\mathrm{capt\ i}}/\partial t = P_i - E_i(T_{s\,i}) - I_i - \mathrm{Ru}_i, \qquad (5)$$

where E_i is the total evaporation for $i \in$ {pav, cova, roof} and the evaporation of the water intercepted by leafs for $i \in$ {vega, vegn}. Here $w_{\mathrm{capt}\ i}$ is in kilograms per squared meter while all fluxes and precipitation are in kilograms per squared meter per second.

2) WATER RUNOFF FROM THE RESERVOIRS Ru_i

When $w_{\mathrm{capt}\ i}$ attains the maximum storage capacity $w_{\mathrm{capt\ max}\ i}$ of the reservoir i, the additional intercepted water runs off. As in ISBA, for vegetation $w_{\mathrm{capt\ max}\ i}$ depends on a maximum water height $h_{\mathrm{max}\ i}$, which depends on vegetation type and the leaf area index LAI_i to account for the foliage interception surface, while for the urban surfaces $h_{\mathrm{max}\ i}$ is an empirical parameter for each type of roof and pavement material,

$$w_{\mathrm{capt\ max}\ i} = \rho_w \,\mathrm{LAI}_i\, h_{\mathrm{max}\ i} \quad \text{for} \quad i \in \{\mathrm{vega}, \mathrm{vegn}\} \tag{6a}$$

and

$$w_{\mathrm{capt\ max}\ i} = \rho_w h_{\mathrm{max}\ i} \quad \text{for} \quad i \in \{\mathrm{pav}, \mathrm{cova}, \mathrm{roof}\}, \tag{6b}$$

where ρ_w is water density.

For roofs and paved surfaces, Ru_i includes the water runoffs to the DN $\mathrm{Ru}_{\mathrm{netw}\ i}$ and to the neighboring surface $\mathrm{Ru}_{\mathrm{neig}\ i}$,

$$\mathrm{Ru}_{\mathrm{netw}\ i} = \mathrm{r}_{\mathrm{netw}\ i}\, \mathrm{Ru}_i^* \quad \text{and} \tag{7a}$$

$$\mathrm{Ru}_{\mathrm{neig}\ i} = (1 - r_{\mathrm{netw}\ i})\, \mathrm{Ru}_i^*, \tag{7b}$$

where $i \in \{\mathrm{pav}, \mathrm{roof}\}$, $r_{\mathrm{netw}\ i}$ is the surface fraction connected to the DN, and Ru_i^* is the water runoff from the whole surface i, that is, for paved surfaces between and under the vegetation.

The water runoff from roofs that are not connected to the DN goes usually to the bare soil located between vegetation elements, or eventually to the paved surfaces. First $\mathrm{Ru}_{\mathrm{pav}}$ goes to the paved surfaces located under the vegetation cova; when this last surface reservoir is full, the runoff from all paved surfaces $\mathrm{Ru}_{\mathrm{pav}}^*$ goes to the DN and/or to the neighboring surfaces, depending on $r_{\mathrm{netw}\ i}$ value. The runoff from paved surfaces that are not connected to the DN goes primarily to the bare soil located between the sparse vegetation elements,

$$\mathrm{Ru}_{\mathrm{pav}}^* = \mathrm{Ru}_{\mathrm{cova}} f_{\mathrm{vega}} / (f_{\mathrm{pav}} + f_{\mathrm{vega}}). \tag{8}$$

3) SURFACE WATER CONTRIBUTIONS P_i

For the vegetation and roofs P_i is equal to the precipitation and watering rate P.

The surface water contributions to paved surfaces without vegetation P_{pav} are precipitation and water runoff from roofs if there is no bare soil,

$$P_{\mathrm{pav}} = P + (f_{\mathrm{roof}}/f_{\mathrm{pav}})\mathrm{Ru}_{\mathrm{neig\ roof}} \quad \text{if} \quad f_{\mathrm{nat}} + f_{\mathrm{vegn}} = 0 \quad \text{and} \quad f_{\mathrm{bare}} = 0, \tag{9a}$$

$$P_{\mathrm{pav}} = P \quad \text{otherwise.} \tag{9b}$$

The contributions to paved surfaces located under the vegetation P_{cova} are the water runoffs from the overlaying vegetation $\mathrm{Ru}_{\mathrm{vega}}$ from the other paved surfaces $\mathrm{Ru}_{\mathrm{pav}}$ and from the roofs when there is no bare soil and if the paved surfaces are entirely covered by vegetation,

$$P_{\mathrm{cova}} = \mathrm{Ru}_{\mathrm{vega}} + (f_{\mathrm{pav}}/f_{\mathrm{vega}})\mathrm{Ru}_{\mathrm{pav}} + (f_{\mathrm{roof}}/f_{\mathrm{vega}})\mathrm{Ru}_{\mathrm{neig\ roof}}$$

$$\text{if } f_{\mathrm{nat}} + f_{\mathrm{vegn}} = 0 \quad \text{and} \quad f_{\mathrm{bare}} = 0 \quad \text{and} \quad f_{\mathrm{pav}} = 0 \quad \text{and} \quad f_{\mathrm{vega}} \neq 0, \tag{10a}$$

$$P_{\mathrm{cova}} = \mathrm{Ru}_{\mathrm{vega}} + (f_{\mathrm{pav}}/f_{\mathrm{vega}})\mathrm{Ru}_{\mathrm{pav}} \quad \text{otherwise.} \tag{10b}$$

4) EVAPORATION FLUXES E_i

The evaporation fluxes E_i from urban (roofs and paved surfaces) and vegetation reservoirs are determined in the same way:

$$E_i = \rho_{\mathrm{air}} \delta_i [q_{v\,\mathrm{sat}}(T_{s\,i}) - q_{v\,\mathrm{ref}}] R_{\mathrm{aq}}^{-1} \quad \text{if} \quad w_{\mathrm{capt}\ i} > 0, \tag{11}$$

where $\mathrm{q}_{v\,\mathrm{sat}}(T_{s\,i})$ and $\mathrm{q}_{v\,\mathrm{ref}}$ are the specific humidities at the surface and at a reference level in the atmosphere, usually the first grid level, and R_{aq} is the canopy aerodynamic resistance. Deardorff's (1978) concept of vegetation fraction covered by intercepted water has been extended here to urban surfaces:

$$\delta_i = (w_{\mathrm{capt}\ i}/w_{\mathrm{capt\ max}\ i})^{2/3} \quad \text{for} \quad q_{v\,\mathrm{sat}}(T_{s\,i}) \geq q_{v\,\mathrm{ref}}\,(\text{evaporation}) \quad \text{and} \tag{12a}$$

$$\delta_i = 1 \quad \text{for} \quad q_{v\,\mathrm{sat}}(T_{s\,i}) < q_{v\,\mathrm{ref}}\,(\text{condensation}). \tag{12b}$$

For simplicity, the evaporation flux from paved surfaces that are located under the vegetation is neglected, $E_{\mathrm{cov}\,a} = 0$. For bare soils (bare and nat) Eq. (11) is altered when the soil is undersaturated with relative humidity. For vegetation covers, the transpiration flux adds to the evaporation to form the evapotranspiration flux. The vegetation transpiration and relative humidity are computed in the same way as in the original ISBA model.

5) WATER INFILTRATION IN THE SOIL I_i

The water infiltration depends on the surface material water infiltration capacity K_i ($\mathrm{m\ s^{-1}}$),

$$I_i = \rho_w K_i \quad \text{for} \quad i \in \{\mathrm{pav}\}. \tag{13}$$

The water infiltration is neglected for the surfaces of roofs and vegetation.

6) WATER CONTENT OF SURFACE LAYERS w_i

The force–restore budget equations of the surface layers under bare and nat surfaces are identical to those of ISBA-3L,

$$\partial w_i/\partial t = C_{1i}\rho_w^{-1}d_1^{-1}P_i - C_2\tau^{-1}(w_i - w_{\rm eq}) \quad \text{for} \quad i \in \{\text{bare, nat}\}, \tag{14}$$

where $w_{\rm eq}$ is the surface layer water content at equilibrium between capillarity and gravity forces and d_1 is the layer thickness; C_{1i} and C_2 are humidity transfer coefficients that have been calibrated against a multilayer soil moisture model (see Noilhan and Mahfouf 1996). The first term on the right-hand side of Eq. (14) represents the influence of surface atmospheric flux forcing that evolves at short time scales, and the second term takes into account the restore toward deep soil content, that is, the diffusivity of water in the soil, evolving more slowly with time. The equilibrium $w_{\rm eq}$ is computed with Clapp and Hornberger's (1978) soil hydraulic parameterization,

$$w_{\rm eq} = w_2 - aw_{\rm sat}(w_2/w_{\rm sat})^c[(1 - w_2/w_{\rm sat})^{8c}], \tag{15}$$

where $w_{\rm sat}$ is the saturated volumetric water content, w_2 is the volumetric water content of the root zone layer, and a and c are empirical parameters.

The water contributions P_i are precipitation plus watering P and water runoff from the neighboring surfaces. Water runoff goes first to the soil between vegetation elements (nat), and second to the bare soil without vegetation (bare). Evaporation E_i is the only water loss;

$$P_{\rm nat} = [P - E_{\rm nat}(T_{\rm s\,nat})]f_{\rm nat}/f_{\rm nv} + {\rm Ru}_{\rm vegn}f_{\rm vegn}/f_{\rm nv} + {\rm Ru}_{\rm neig\,roof}f_{\rm roof}/f_{\rm nv} + {\rm Ru}_{\rm neig\,pav}(f_{\rm pav} + f_{\rm vega})/f_{\rm nv} \tag{16}$$

where $f_{\rm nv} = f_{\rm nat} + f_{\rm vegn}$,

$$P_{\rm bare} = P - E_{\rm bare}(T_{\rm s\,bare}) + {\rm Ru}_{\rm neig\,roof}f_{\rm roof}/f_{\rm bare} + {\rm Ru}_{\rm neig\,pav}(f_{\rm pav} + f_{\rm vega})/f_{\rm bare} \quad \text{if} \quad f_{\rm nat} + f_{\rm vegn} = 0, \tag{17a}$$

$$P_{\rm bare} = P - E_{\rm bare}(T_{\rm s\,bare}) \quad \text{otherwise.} \tag{17b}$$

7) WATER CONTENT OF THE ROOT ZONE LAYER w_2

This layer is common under all nonwater surfaces of a cell. The water content budget equation is

$$\partial w_2/\partial t = \rho_w^{-1}d_2^{-1}P_2 - D_2 - K_2, \tag{18}$$

where d_2 and d_3 are the root zone and deep soil layer thickness, respectively. The first term on the right-hand side of (18) is the atmospheric forcing, D_2 the restore term to equilibrium between the soil layers by vertical moisture diffusion, and K_2 the gravitational drainage of soil water.

The atmospheric contributions P_2 are the net water content of the surface layers (precipitation and watering plus runoff minus evaporation) and the infiltration through the paved surfaces while the losses are vegetation transpirations $E_{\rm tr\,vegn}$ and $E_{\rm tr\,vega}$ transferred through the root system, and from the evaporation from bare soils $E_{\rm nat}$ and $E_{\rm bare}$,

$$P_2 = f_{\rm nv}P_{\rm nat} + f_{\rm bare}P_{\rm bare} + f_{\rm pav}I_{\rm pav} + f_{\rm vega}I_{\rm cova} - f_{\rm vegn}E_{\rm tr\,vegn}(T_{s\,\rm vegn}) - f_{\rm vega}E_{\rm tr\,vega}(T_{s\,\rm vega}). \tag{19}$$

The vegetation transpiration depends on the stomatal resistance, which is parameterized as a minimum stomatal resistance $R_{s\,\rm min\,vegn}$ ($R_{s\,\rm min\,vega}$) with additive factors depending on the solar radiation, soil moisture, vapor pressure deficit, and air temperature (Jacquemin and Noilhan 1990). Here $R_{s\,\rm min\,vegn}$ ($R_{s\,\rm min\,vega}$) is scaled in the model for the whole canopy.

The parameterizations of the vertical soil moisture diffusion term D_2

$$D_2 = C_4\tau^{-1}(w_2 - w_3) \tag{20}$$

and the gravitational drainage term K_2 (activated when the soil water content is larger than the field capacity $w_{\rm fc}$)

$$K_2 = C_3\tau^{-1}(d_3/d_2)\max[0, (w_2 - w_{\rm fc})] \tag{21}$$

are those of the recent ISBA-3L of Boone et al. (1999), where C_3 and C_4 are calibrated coefficients.

8) WATER CONTENT OF THE DEEP SOIL LAYER w_3

The deep-soil-layer budget equation was introduced by Boone et al. (1999) to include the gravitational and diffusion exchanges with the root layer and drainage out of the system K_3,

$$\partial w_3/\partial t = d_2(d_3 - d_2)^{-1}(K_2 + D_2) - K_3, \tag{22}$$

where K_3 is calculated in the same way as K_2,

$$K_3 = C_3\tau^{-1}d_3(d_3 - d_2)^{-1}\max[0, (w_3 - w_{\rm fc})]. \tag{23}$$

3. Field experiments

a. Rural sites

The HAPEX-MOBILHY (André et al. 1986) experiment took place in 1986 in southwestern France, which

FIG. 2. Aerial view of the Rezé site. The black continuous line indicates the limits of the catchment drained by the drainage network in the right-hand corner.

is characterized by a temperate climate. The surface is largely covered by homogeneous soybean crop fields starting to grow in May and harvested at the end of September. From a texture analysis, the soil was characterized as loamy and assumed homogeneous up to 1.6 m in depth. The HAPEX-MOBILHY comparison concerns only the data obtained over the Caumont site; the meteorological data and the volumetric water content in 16 soil layers, each one 10 cm thick down to 1.6 m, were recorded during the full year, whereas the net radiation, sensible heat flux in the air, and conduction heat flux in the soil were measured from a Système Automatique de Mesure de l'Evapotranspiration Régionale (SAMER) station during an intense observation period (IOP) from 28 May to 3 July. The latent heat flux was not measured but deduced as the energy balance residual. As reported by Shao and Henderson-Sellers (1996), the accuracy of the flux measurements was assessed by Goutorbe (1991) to be around 15% at a short time scale.

The EFEDA (Bolle et al. 1993) experiment took place in southeastern Spain in June 1991 over three sites: Tomellos, Barrax, and Belmonte. We focus here only on the dataset from the Belmonte site, characterized by sparse, small natural scrub under dry Mediterranean climate. The data correspond to the period from 8 to 13 June 1991. The wind was measured at 12 m and the data have been interpolated down to 2 m using the logarithmic profile with $z_0 = 0.02$ m. As for the HAPEX-MOBILHY campaign, energy flux and atmospheric forcing were measured from SAMER stations. The soil was characterized as loamy and assumed homogeneous up to 1.4 m in depth where soil moisture was measured.

b. Suburban sites

The suburban catchment of the Rezé site has been instrumented since the early 1990s (Berthier et al. 1999). The site is a housing estate with a homogeneous distribution of surface types composed of small houses with one or two stories, surrounded by gardens and connected to an asphalt road (Fig. 2). The natural and artificial surfaces are balanced, 55.5% and 44.5%, respectively, including 16.8% buildings and 27.7% pavement. Most artificial surfaces, 92% of the roofs and 80% of the paved surfaces, are connected to the DN. The buildings are typical of western France—individual houses with predominant tile roofs. Natural surfaces are bare soil with vegetation. The vegetation is very heterogeneous in size and species, with grass, shrubbery, floral zones, and various types of evergreen and deciduous trees, some of which are higher than the buildings. A granulometric study classified the soil as "silt loam" with 4% clay and 38% sand. The neighborhoods are similar suburban districts except for the rural area with trees on the west. The catchment extends over 4.7 ha with a mean slope of 2%, as delineated by the black line in Fig. 2, and the DN outlet instrumentation is at the left-hand-side corner.

The site roughness length z_0 and displacement height z_d have been first computed with the morphometric parameterizations of Raupach (1992) and Bottema (1997). The site is certainly too small for expecting the wind field to be in equilibrium with its own roughness higher than a few meters. For most of the year, it is more probable that the flow is established with a roughness averaging those of the site itself and of its surroundings, or that the flow is too disturbed by the high-

est roughnesses to be fully established; then, the wind velocity probably does not present a logarithmic profile. Thus, the determination of the relevant roughness parameters becomes complex. However, given the large differences between the values of z_0 and z_d provided by the various parameterizations (see Grimmond et al. 1998), it has been decided to use an average of the values provided by Bottema's and Raupach's formulas (Table 1).

The set of experimental data includes precipitation (rain gauge), water flow at the DN outlet (flowmeter), and soil water content 1.5 m under a lawn surface (tensiometer). These data are available since 1991 with a 1-min time step for precipitation and the DN flow, and since 1995 with a 1-h time step for the soil water content (Berthier et al. 1999). Data are missing for only a few periods, especially for the soil water content. Meteorological data were measured at the Météo-France station located 5 km to the west of the site with the standard procedures, wind speed at 10 m, air temperature and water vapor pressure at 1.2 m, atmospheric pressure, and incoming solar radiation.

For the numerical simulations, the meteorological variables were assumed identical at high elevations over the meteorological and Rezé sites. The wind speed, air temperature, and air specific humidity (deduced from the water vapor pressure and the atmospheric pressure) were extrapolated to the reference level (50 m) with an algorithm accounting for the atmospheric stability and assuming site-adapted pseudo-logarithmic profiles (Dupont 2001).

4. Simulations

For the three sites, the model is used in stand-alone mode, by constraining the atmospheric inputs (pressure, temperature, humidity, wind speed, precipitation, and radiation) to follow the observations. Because the site land covers are well mixed and SM2-U does not compute horizontal water exchanges between cells, the sites are represented by only one cell. The computational domain is one column 4, 4, and 100 m high in the air (2 times the measurement height), and 1.6, 1.4, and 3 m deep in the soil, for the HAPEX-MOBILHY,

TABLE 1. Parameters used in the SM2-ISBA and SM2-U simulations.

Symbol	Variable	HAPEX-MOBILHY	EFEDA, Belmonte	Rezé
f_{vegn}	Vegetation cover rate	0,[a] 0.5,[b] 0.9[c]	0.4	0.416
z_0	Roughness length (m)	0.01,[a] 0.05,[b] 0.15[c]	0.02	0.13
z_{0h}	Heat roughness length (m)	$0.1z_0$	$0.1z_0$	$0.1z_0$
z_d	Displacement height (m)	0	0	3.25
α	Vegetation albedo	0.2	0.1	0.13
ϵ	Emissivity	1.0	1.0	0.96
C_T, C_{Tveg}	Vegetation heat capacity (10^{-3} m^{-2} K J^{-1})	$1^{\text{SM2-ISBA}}$, $0.15^{\text{SM2-U}}$	$1^{\text{SM2-ISBA}}$, $0.02^{\text{SM2-U}}$	0.02
LAI_n	Leaf area index	0,[a] 1,[b] 3[c]	1.5	1,[a] 2,[b] 3[c]
$h_{\text{max vegn}}$	Max water storage height (mm)	0.2	0.2	0.2
$h_{\text{max roof}}$	Max roof water storage height (mm)	—	—	0.5
$\text{h}_{\text{max pav}}$	Max pavement storage height (mm)	—	—	3.5
$r_{\text{netw roof}}$	DN-connected roof fraction	—	—	0.92
$r_{\text{netw pav}}$	DN-connected pavement fraction	—	—	0.80
K_{pav}	Pavement infiltration capacity (m s^{-1})	—	—	7.5×10^{-8}
$R_{s\ \text{min vegn}}$	Min stomatal resistance (s m^{-1})	80	$120^{\text{SM2-ISBA}}$, $40^{\text{SM2-U}}$	80
X_{clay}	Soil composition, clay (%)	17	19	4
X_{sand}	Soil composition, sand (%)	37	43	38
d_1	Surface layer depth (m)	0.1	0.1	0.1
d_{soil}	Soil layer depth (m)	1.6 ($d_2 = 1.1$)	1.4 ($d_2 = 0.9$)	3.0 ($d_2 = 1.5$)
w_{sat}	Saturation volumetric water content	0.446	0.451	0.45
w_{wilt}	Wilt volumetric water content	0.150	0.140	0.074
w_{fc}	Field capacity	0.320	0.240	0.380
a	Coef in w_{geq} parameterization	0.148	0.148	0.347
c	Coef in w_{geq} parameterization	6.0	6.0	4.0
b	Slope of retention curve	5.66	5.39	4.05
$C_{\text{G sat}}$	Thermal coef at saturation (K m^{-2} J^{-1})	4.111×10^{-6}	4.111×10^{-6}	4.053×10^{-6}
$C_{1\ \text{sat}}$	C_1 value at saturation	0.191	0.191	1.072
$C_{2\ \text{ref}}$	C_2 value for $w_2 = w_{\text{sat}}/2$	0.8	0.8	3.7
C_3	Third-layer drainage coefficient	0.19	0.19	1.7

[a] From January to April, and from October to December.
[b] May.
[c] From June to September.

EFEDA, and Rezé simulations, respectively. The thickness of the soil surface layer is 0.1 m and that of the root zone layer is 1.6 and 1.4 m in the two-layer initial simulations of HAPEX-MOBILHY and EFEDA, respectively, and 1.1, 0.9, and 1.5 m in the three-layer simulations of HAPEX-MOBILHY, EFEDA, and Rezé, respectively. Because SM2-ISBA has two soil layers, SM2-U was also driven with two layers during the first model comparisons. The model parameters are summarized in Table 1. The model calibration for the two on both rural campaigns is the same as that of ISBA as reported by Noilhan and Planton (1989), Jacquemin and Noilhan (1990), Noilhan and Mahfouf (1996), and Boone et al. (1999) for HAPEX-MOBILHY and by Braud et al. (1993), Giordani et al. (1996), and Noilhan and Mahfouf (1996) for EFEDA. The canopy parameters such as roughness length, fractional coverage, leaf area index, vegetation height, albedo, and emissivity were estimated from observations.

For the Rezé site, the selected values of the empirical parameters either result from the site observations of Berthier et al. (1999), or from technical handbooks [see Guilloteau 1999; Berthier 1999; Berthier et al. 2004; and the discussion in section 5b(3)]. The anthropogenic heat fluxes resulting from vehicles are neglected here because of the very light traffic within the housing estate.

For all sites, the model soil parameters (hydraulic properties) were computed using a set of relationships based on the soil texture (Noilhan and Mahfouf 1996; Boone et al. 1999).

Although it represents the most important vegetation parameter controlling the latent heat flux, the minimum stomatal resistance ($R_{s\,\mathrm{min\,vegn}}$) that appears in the transpiration flux (not detailed above) is difficult to measure within a reasonable accuracy (Boone et al. 1999). Increasing $R_{s\,\mathrm{min\,vegn}}$ reduces the vegetation transpiration, and $R_{s\,\mathrm{min\,vegn}}$ depends widely on the plant canopy type. Typical values are around 40 s m^{-1} for a live crop and 100 s m^{-1} for a forest (Jacquemin and Noilhan 1990); however, $R_{s\,\mathrm{min\,vegn}}$ may reach higher values ($\sim$500 s m^{-1}) when crops experience maturation or senescence (Noilhan and Planton 1989; Noilhan and Mahfouf 1996). Hence, because of the whole uncertainties on the $R_{s\,\mathrm{min\,vegn}}$ value, this parameter is usually treated as a calibration parameter in soil models (Boone et al. 1999). For HAPEX-MOBILHY $R_{s\,\mathrm{min\,vegn}}$ was set to 80 s m^{-1} for both models. Noilhan and Planton (1989) originally used 40 s m^{-1} while Boone et al. (1999) "recalibrated" this parameter to optimize the three-layer fluxes of HAPEX-MOBILHY and found an optimum of 150 s m^{-1}, which seems to be a very high value usually attributed to forests. For EFEDA Noilhan and Mahfouf (1996) originally used 120 s m^{-1}; here, $R_{s\,\mathrm{min\,vegn}}$ was set to 150 s m^{-1} in SM2-ISBA and 80 s m^{-1} in SM2-U. A value of 80 s m^{-1} may be still too high for soybean and scrub canopies, but this is the value that Monteith (1976) proposed for mature crops. For Rezé, $R_{s\,\mathrm{min\,vegn}}$ was set at 80 s m^{-1}.

There is also some uncertainty in the value of the vegetation surface resistance to the atmospheric forcing $C_{T\,s\,\mathrm{vegn}}$. Initially, Deardorff (1978) used a value of 0.0096 K m^{-2} J^{-1} for a wheat crop. Noilhan and Planton (1989) suggested a value of 10^{-3} K m^{-2} J^{-1} in the first description of ISBA, then Noilhan and Mahfouf (1996) suggested 2×10^{-5} K m^{-2} J^{-1}. The vegetation surface resistance controls the plant heat storage by the vegetation; a higher value of $C_{T\,s\,\mathrm{vegn}}$ reduces the conduction heat flux. Here, in SM2-ISBA, $C_{T\,s\,\mathrm{vegn}}$ was set to the initial value proposed by Noilhan and Planton (1989), whereas in SM2-U it was calibrated to 0.15 10^{-3} m^2 K J^{-1} for HAPEX-MOBILHY, and 2 10^{-5} m^2 K J^{-1} for EFEDA and Rezé.

The initial values of the soil water content and temperature were prescribed from available observations in EFEDA: $T_{\mathrm{soil}} = 298.16$ K, $w_{\mathrm{nat}} = 0.054$, $w_2 = w_3 = 0.153$. For HAPEX-MOBILHY, the simulations were performed over 2yr, and the first year was used as an initialization period for the model to reach equilibrium in order to minimize the influence of the initial conditions in the second year. For Rezé, the simulations extend over 6 yr from 1993 to 1998 and the full year 1993 was used as an initialization period for SM2-U.

The model performances on the rural sites are quantified by means of the root-mean-square error (rmse), defined for a variable Φ by

$$\mathrm{rmse} = \left[n^{-1} \sum_{i=1}^{n} (\Phi_{\mathrm{simulation,\,i}} - \Phi_{\mathrm{observation,\,i}})^2 \right]^{1/2}, \tag{24}$$

where n is the total number of measurements during the IOP.

The model results on Rezé site are compared with the measurements of the DN water flow with a 1-h time step, using the "Nash" (Nash and Sutcliffe 1970) and total volume criteria (%),

$$C_{\mathrm{Nash}} = 100 \left\{ 1 - \sum_{i=1}^{n} [Q_{\mathrm{sim}}(t_i) - Q_{\mathrm{obs}}(t_i)]^2 \Big/ \sum_{i=1}^{n} [Q_{\mathrm{obs}}(t_i) - \overline{Q_{\mathrm{obs}}}]^2 \right\} \quad \text{and} \tag{25}$$

$$C_{\mathrm{Qtot}} = 100 \left\{ \sum_{i=1}^{n} [Q_{\mathrm{sim}}(t_i) - Q_{\mathrm{obs}}(t_i)] \Big/ \sum_{i=1}^{n} Q_{\mathrm{obs}}(t_i) \right\}, \tag{26}$$

where Q_{obs} is the observed water flow ($m^3\ h^{-1}$), $\overline{Q_{obs}}$ is its mean value over the stormy events of the period, Q_{sim} is the simulated water flow, and n is the total number of measurements during the stormy events. The Nash criterion evaluates the simulation error relative to the natural variation in the observed values while the volume criterion evaluates the bias. Perfect simulations with no bias would yield $C_{Nash} = 100$ and $C_{Qtot} = 0$. The criteria are used only for the periods of the 1994–98 stormy events because of the uncertainty in the DN water flow measurements during dry periods.

5. Results and discussion

a. Rural site

Figure 3 compares the measured and simulated fluxes during the IOP of the HAPEX-MOBILHY experiment. On the whole the net radiation cycles are correctly reproduced by both models (Fig. 3a), but they both overestimate it in the daytime. Also, during some nights both models underestimate the negative net radiation. The sensible heat flux simulations are quite similar with the two models (Fig. 3b); both models overestimate the nighttime negative fluxes. The storage heat flux is quite well estimated with both models, considering its moderate amplitude (Fig. 3c); the high-frequency fluctuations in the simulations (lower in SM2-U) may be because of the fact that the stored heat was measured in the soil only while the simulated fluxes include also the heat stored in the vegetation, which is small but rapidly varying. The experimental latent heat flux is actually the energy imbalance, and therefore includes also the experimental errors (Fig. 3d); the two models reproduce it well on the average, with a clear reluctance to simulate the nighttime negative fluxes resulting from condensation. During daytime SM2-U yields usually a lower latent heat flux than does SM2-ISBA, often in better agreement with the observations.

The model allows a finer analysis, separating the various contributions that are not separated in the measurements, such as those of the bare soil and of the vegetation (Fig. 4). The vegetation transpiration (not shown) is higher in SM2-U simulations than in those of SM2-ISBA, while the total evapotranspiration from the vegetation layer is higher with SM2-ISBA, leading to the daytime overestimation. A larger difference is observed in bare soil evaporation (Fig. 4a), which is twice as large with SM2-ISBA as with SM2-U, although this does not appear that much in the average fluxes (Fig. 3d) because the bare soil represented only 10% of the surface during this period (Table 1). This difference is enlightened by the large surface temperature differences between the bare soil and the vegetation (Fig. 4b). Because of the large vegetation cover the average surface temperature is very close to that of the vegetation, which is much higher in the daytime (and is often much lower in the nighttime). Because in SM2-ISBA the aerodynamic surface fluxes are computed at the average surface temperature the bare soil evaporation appears to be largely overestimated. A separated analysis of the energy budget components obtained with SM2-U (not shown) indicates that the latent heat flux by evaporation over the interspersed bare soil is very high during daytime, as large as, or even larger than, the net radiation, while the soil storage heat flux is small, resulting in often negative sensible heat fluxes. Over the vegetation layer the net radiation is slightly lower during the daytime and, the heat storage being negligible, it is shared out by the sensible and evapotranspiration latent heat fluxes approximately in the proportion of 2:3. At night the negative net radiation is exactly compensated by the negative sensible heat flux.

From this analysis it results that the bare soil latent heat flux (from evaporation) may be dangerously overestimated by SM2-ISBA's use of a unique surface temperature when the soil humidity is available, although this does not appear strikingly here in the average flux because of its low surface cover. The separate calculation of surface temperatures by cover modes does not appear to alter the overall performances of the model; on the contrary, it tends certainly to improve the component contributions.

The measured and simulated water contents in the soil are compared in Fig. 5 over all of 1986. In Fig. 5a the total water content of the 1.6-m-thick layer is compared with the model simulations with two soil layers. The simulations of the two models are identical during the winter/spring period when the soil is saturated by frequent rains; they slightly diverge during the drier summer period because of the above-mentioned overestimation of the evaporation by SM2-ISBA. The better performance of SM2-U is shown by the water content rmse, which is reduced by 10% (Table 2). In Fig. 5b the measured volumetric water content in the root zone (1.1 m) and deep soil (1.1–1.6 m) layers are compared with the simulation with the three-soil-layer model. In the average the simulations are improved by the third soil layer implementation, although the contents of each of the two layers are not well simulated; the improvement appears to be caused by the third layer's temporary water reserve rather than by the improved layer parameterizations. This figure may be compared with Fig. 10 of Boone et al. (1999), which shows a similar agreement with the averaged measurements (SM2-U looks marginally better) but a much better agreement with the separated measurements in the two

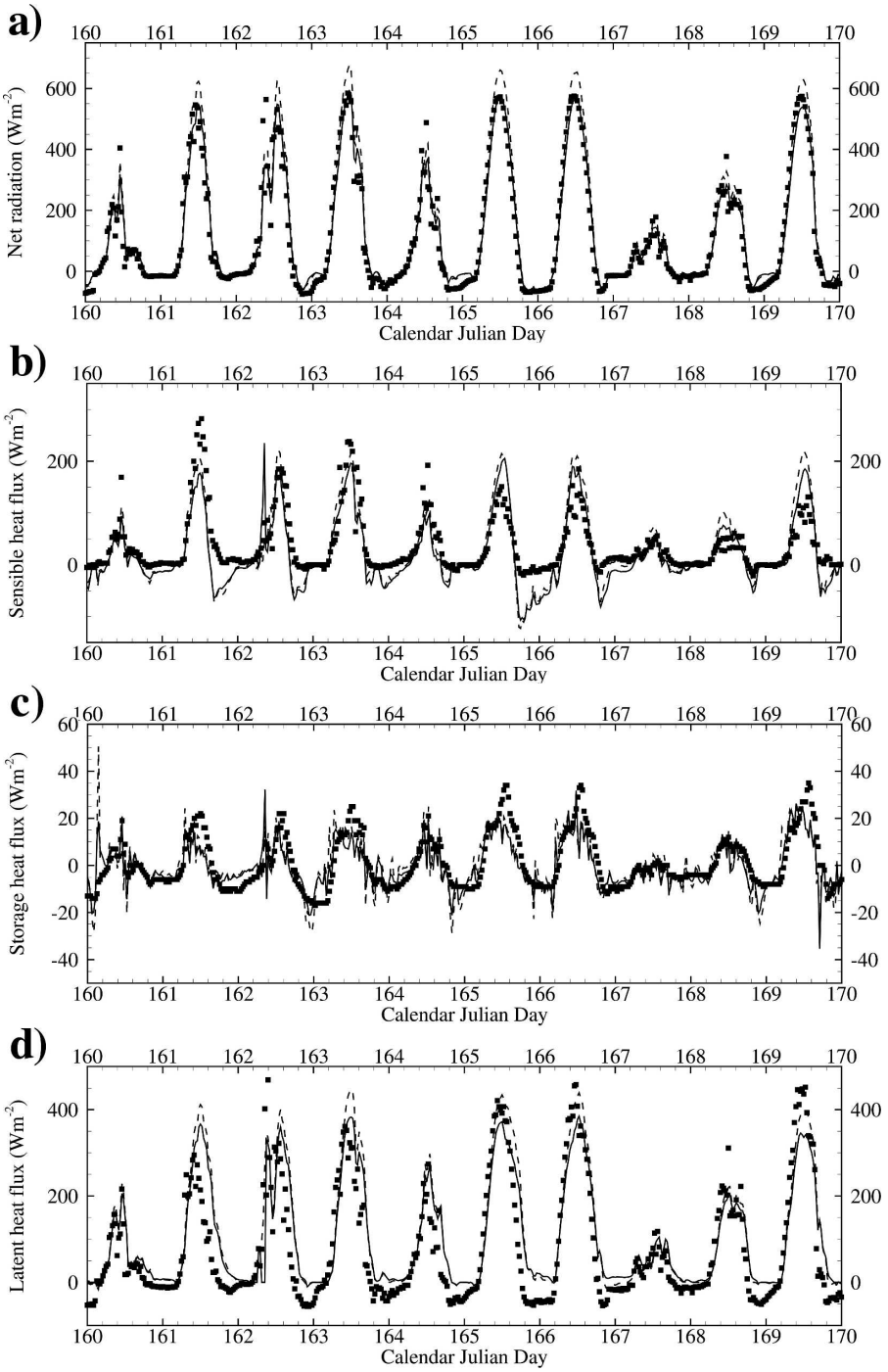

FIG. 3. Model validation for HAPEX-MOBILHY (IOP, 28 May–3 Jun) (a) net radiation, (b) sensible heat flux, (c) soil conduction heat flux, and (d) latent heat flux for the measurements (squares), the SM2-U simulation (solid line), and the SM2-ISBA simulation (dashed line).

layers. This may result from Boone et al.'s (1999) unexplained decision to replace the loamy soil composition (37% sand, 46% silt, 17% clay), adopted in the model intercomparison (Shao and Henderson-Sellers 1996) with a silty, clay loam composition (10% sand, 34% clay) (although they report observation of loamy soil), and from their empirical recalibration of the vegetation minimum stomatal resistance $R_{s\,\mathrm{min\,vegn}}$ to optimize these simulations, yielding the curiously high value of 150 s m^{-1}. When this high value is used, the

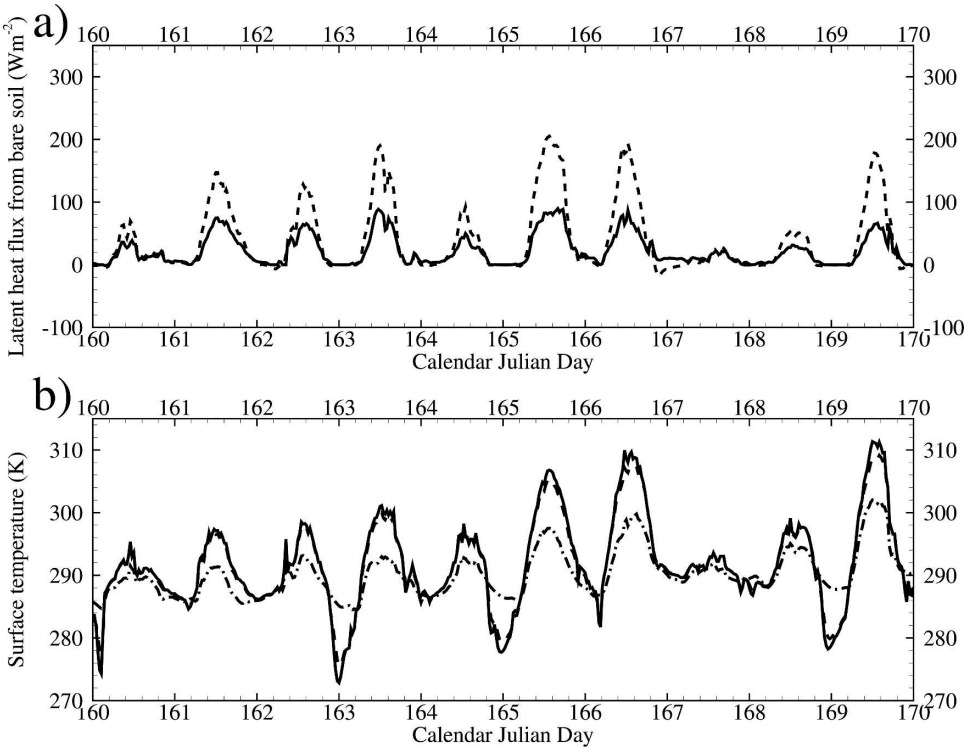

FIG. 4. Model simulation of HAPEX-MOBILHY (IOP, 28 May–3 Jun) (a) bare ground evaporation humidity flux for the SM2-U (solid line) and SM2-ISBA (dashed line) simulations, and (b) surface temperature for SM2-U vegetation (solid line), bare soil temperatures (dash–dot line), and SM2-ISBA mean surface temperature (dashed line).

water content rmse obtained by SM2-U decreases strongly (30%) because the vegetation transpiration is reduced, however, the latent and sensible heat flux rmses increase (Table 2). On the other hand, with a typical crop value of $R_{s\,\mathrm{min\,vegn}}$ (40 sm^{-1}), the vegetation transpiration is largely over-estimated, inducing a high water content rmse, but a better sensible heat flux rmse (Table 2).

The net radiation overestimation by both models may be addressed by increasing the vegetation albedo. Noilhan and Planton (1989) used an albedo of 0.24; here it was set to 0.20, the value adopted in the model intercomparison (Shao and Henderson-Sellers 1996). Hence, with an albedo of 0.30 the net radiation overestimation is removed (Table 2), and the sensible heat flux and water content rmses are reduced by 20% and 22%, respectively, relative to the referenced simulation.

The model validation for the EFEDA campaign is illustrated by Fig. 6. The net radiation is extremely well simulated (Fig. 6a). The sensible heat flux is also well simulated, with a limited midday overestimation by SM2-ISBA and a small underestimation by SM2-U (Fig. 6b). The simulated storage heat fluxes again show high-frequency fluctuations (Fig. 6c) and good average diurnal cycles even at night, except for a clear underestimation of the daytime fluxes by SM2-ISBA; this daytime underestimation is largely reduced by SM2-U, as shown by the 20% reduction of the rmse (Table 2). The simulations of the latent heat fluxes by the two models are quite similar (Fig. 6d) and overestimate the daytime measurements (actually the measurement imbalances). Because the soil was rather dry the vegetation transpiration was limited, and this overestimation may be attributed to the evaporation from the bare soil that occupied here a larger fraction of 60%. We think that this is because of the limiting value of the surface layer humidity transfer coefficient C_1 [see Eq. (14)]. In Noilhan and Planton (1989)

$$C_{1i} = C_{1\mathrm{sat}}(w_{\mathrm{sat}}/w_i)^{1+b/2}, \tag{27}$$

and the maximum value of C_1 is attained when the surface layer reaches the wilt point, that is,

$$C_{1\mathrm{max}} = C_{1\mathrm{sat}}(w_{\mathrm{sat}}/w_{\mathrm{wilt}})^{1+b/2}, \tag{28}$$

where w_{sat}, w_{wilt}, and b depend on soil texture (Noilhan and Planton 1989; Jacquemin and Noilhan 1990). Braud

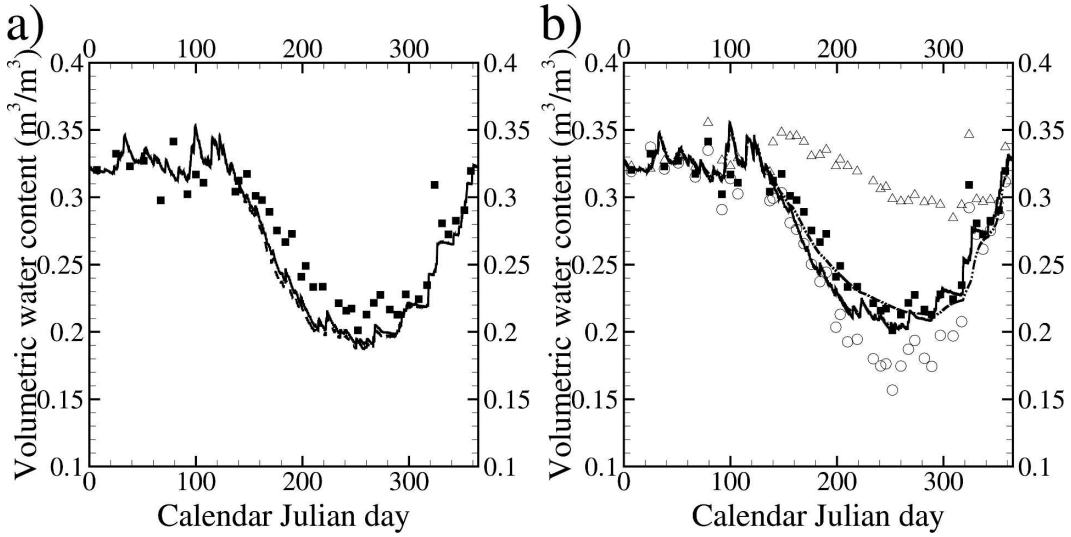

FIG. 5. Model simulation of HAPEX-MOBILHY (year 1986) (a) total soil water content in the 1.6-m-thick soil layer for the measurements (squares), SM2-U simulation (solid line, two soil layers), and SM2-ISBA simulation (dashed line); and (b) volumetric water content of the root zone layer (circles and dash–dot line), deep soil layer (triangles and dashed–dot–dot line), and the average (squares and solid line); the symbols are the measurements and the lines are the simulation with SM2-U three-layer model.

et al. (1993) observed that the evaporation flux of the EFEDA site Barrax was underestimated in ISBA simulations and attributed it to a too low value of $C_{1\,\max}$. An optimum value to match the measurements was found to be 0.45. This value was implemented in SM2-ISBA (Guilbaud 1996) and was used in the present simulations. Actually, this coefficient does not take into account the vapor phase humidity transfer, which is larger than that of the liquid one when the soil is dry. Braud et al. (1993) and Giordani et al. (1996) proposed some improved parameterizations of $C_{1\,\max}$, as discussed by Dupont (2001) for SM2-U implementation. Note that, to improve ISBA heat flux simulation, Giordani et al. (1996) proposed also to reduce the heat roughness length, obtaining an optimum with $z_{0h} = z_0/100$. We observed that this produced erroneous heat flux estimations and that the more commonly observed value $z_{0h} = z_0/10$ (Guilloteau 1999) was retained in SM2-U.

As a provisional conclusion from these validation exercises it is found that in the average the model behavior is not perturbed by the separate calculation of the cover mode energy budget and surface temperature, on the contrary, the performance is most often better with a lower rmse. Even for rural soils the advantage appears clearly because it allows for better identification

TABLE 2. Root-mean-square error of simulations in comparison with IOP observations for the fluxes and all-year observations for the soil water quantity (2L, 3L: two, three soil layers, respectively).

	Rmse	R_n (W m^{-2})	LE (W m^{-2})	G_s (W m^{-2})	H_{sens} (W m^{-2})	Q_{water} (mm)
HAPEX-MOBILHY	SM2-ISBA	65.7	73.5	16.1	48.7	38.7
	SM2-U (2L)	65.2	74.6	12.0	53.8	34.9
	SM2-U (3L)	65.0	74.6	11.9	55.8	31.8
	SM2-U (3L)[a]	59.5	76.3	12.0	44.6	27.2
	SM2-U (3L)[b]	66.8	81.8	11.8	46.7	50.3
	SM2-U (3L)[c]	63.5	80.2	12.1	73.4	24.5
EFEDA, Belmonte	SM2-ISBA	7.6	28.8	38.6	37.4	—
	SM2-U (2L)	12.4	30.0	31.0	27.7	—
	SM2-U (3L)	12.1	31.0	31.0	28.1	—

[a] $\alpha = 0.30$.
[b] $R_{s\,\min\,\text{vegn}} = 40$ s m^{-1}.
[c] $R_{s\,\min\,\text{vegn}} = 150$ s m^{-1}.

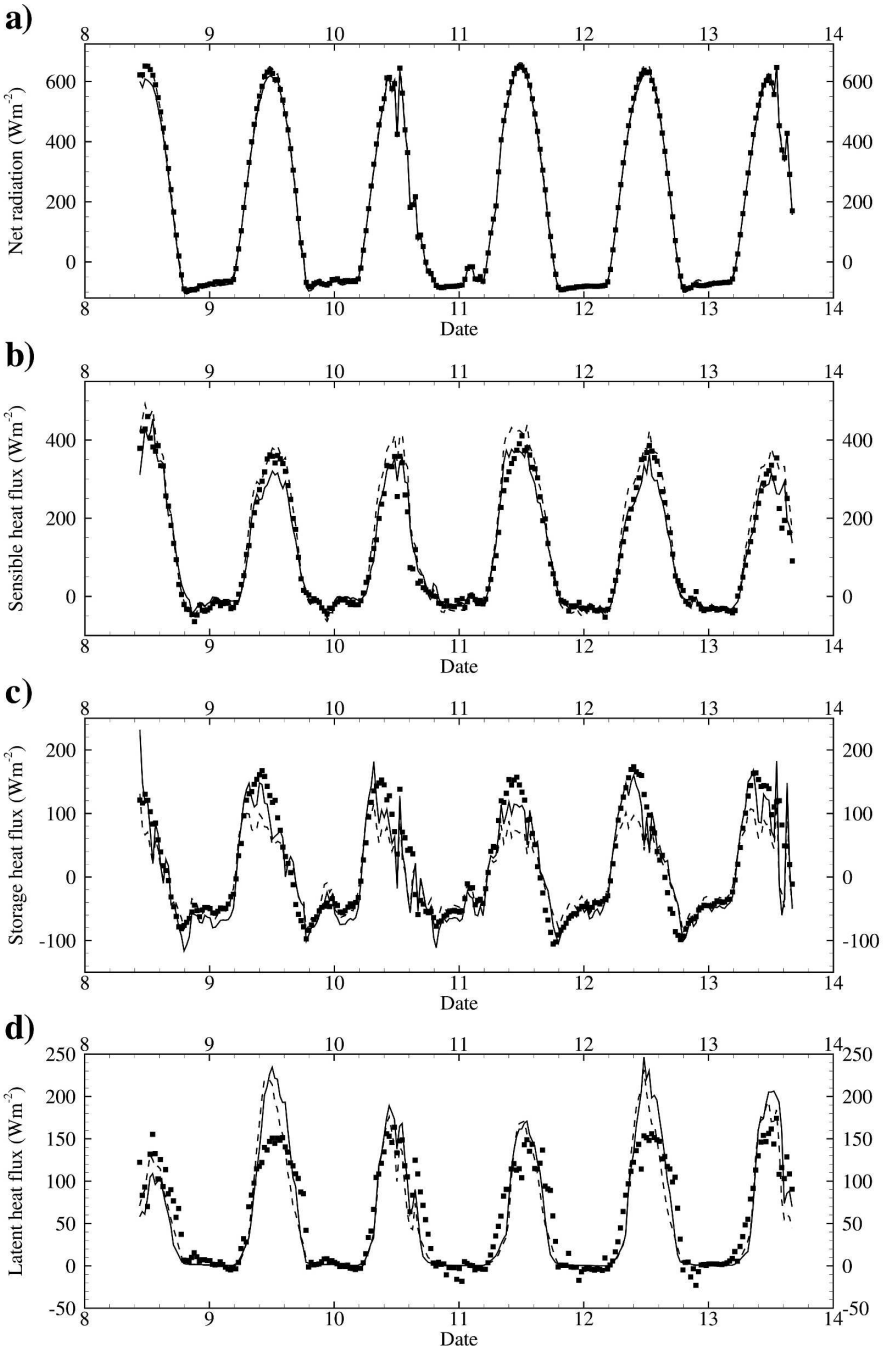

FIG. 6. Model validation for EFEDA (Belmonte, 8–13 Jun 1991) (a) net radiation, (b) sensible heat flux, (c) soil conduction heat flux, and (d) latent heat flux for the measurements (squares), the SM2-U simulation (solid line), and the SM2-ISBA simulation (dashed line).

of the various contributions in the various processes on a more physical basis when high-resolution meteorology and microclimatology are aimed at. Although a large number of works to refine the ISBA model have already been published, the model efficiency appears to be balanced by the large number of empirical parameters and sensitive to several parameters that are still not universally controlled, such as the minimum stomatal resistance and the vegetation surface resistance to the atmospheric forcing. Yet, the quality of its outputs is generally very good, and it seems transposable to urban grounds.

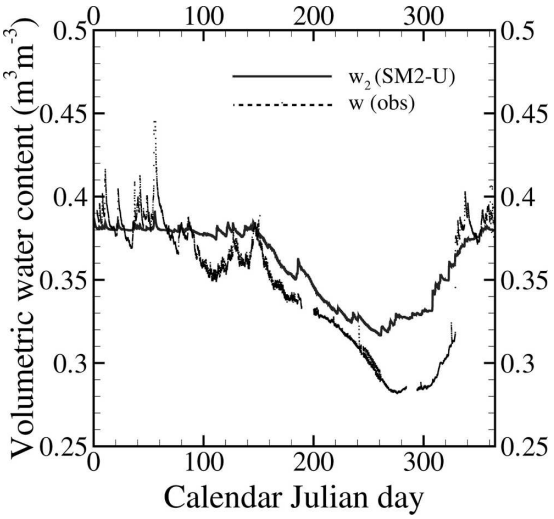

FIG. 7. Comparison of the SM2-U modeled root-zone-layer volumetric water content (w_2) with the measurements at 1.5 m under a lawn surface (Rezé site, year 1996).

b. Suburban site

1) THE REFERENCE SIMULATION

The results of SM2-U reference simulations are first presented at the annual scale, followed by a focus on two stormy events.

In Fig. 7 the simulated volumetric water content of the root zone layer (w_2) is compared with the measurements at −1.5 m during 1996, which is the year with the most complete soil dataset. This comparison is delicate because the measurements document the soil water content at one point, 1.5 m under a natural surface, whereas the SM2-U simulations correspond to the average of the 1.5-m-thick layer under the entire site, including buildings and paved surfaces. This comparison cannot validate the simulation quantitatively but allows us to check the coherence of the annual time variation. Here the finescale time variations are smoothed in the simulations because of the limited water infiltration through artificial surfaces (roads and roofs). The annual cycle simulation is qualitatively good and quantitatively correct during the first 5 months of the year when the soil remains wet because of frequent precipitation and low evaporation, with soil water content close to that of the field capacity. From June to October, when the soil is drying because of the precipitation decrease and the vegetation transpiration, w_2 is always higher than the observations. This can be explained by the sensor location, where the soil drying up by evapotranspiration is the most efficient, whereas the artificial surfaces have no evaporation. Another reason may be an evapotranspiration underestimation by SM2-U resulting from the difficulty parameterizing the heterogeneous site vegetation. Unfortunately, the measurements did not include the surface humidity fluxes. After October the soil becomes increasingly wet and the simulation follows the observed humidity increase.

TABLE 3. Nash and total volume criteria of SM2-U and UHE simulations of the water flow in the DN (Rezé site for the period of 1994–98, hourly data); SM2-U*, simulation with soil water infiltration forcing.

Models	C_{Nash}	C_{Qtot}
SM2-U	77.3%	−6.8%
UHE	77.7%	−3.2%
SM2-U*	78.5%	+1.9%

The Nash and volume criteria for the DN flow simulations over the period of 1994–98 are equal to 77.3% and −6.8%, respectively, showing that SM2-U underestimates the flux but simulates correctly its time varia-

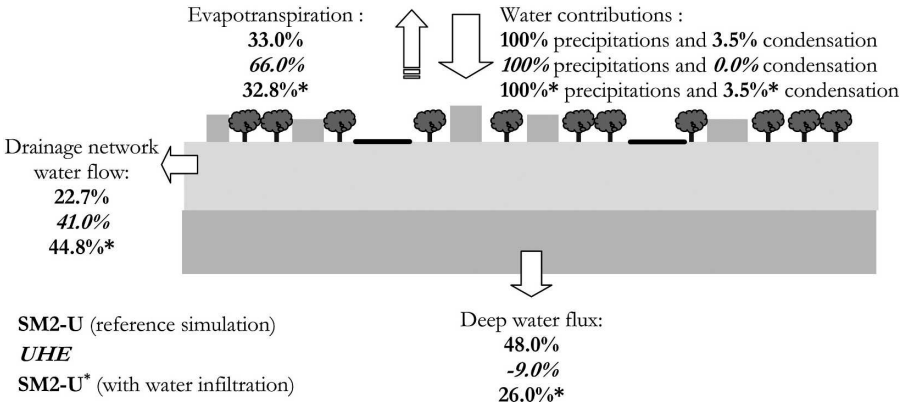

FIG. 8. Water fluxes (percent of the precipitation) in the Rezé site simulations for the period of 1994–98 with SM2-U (right numbers), UHE (numbers in italics), and SM2-U* (numbers with *).

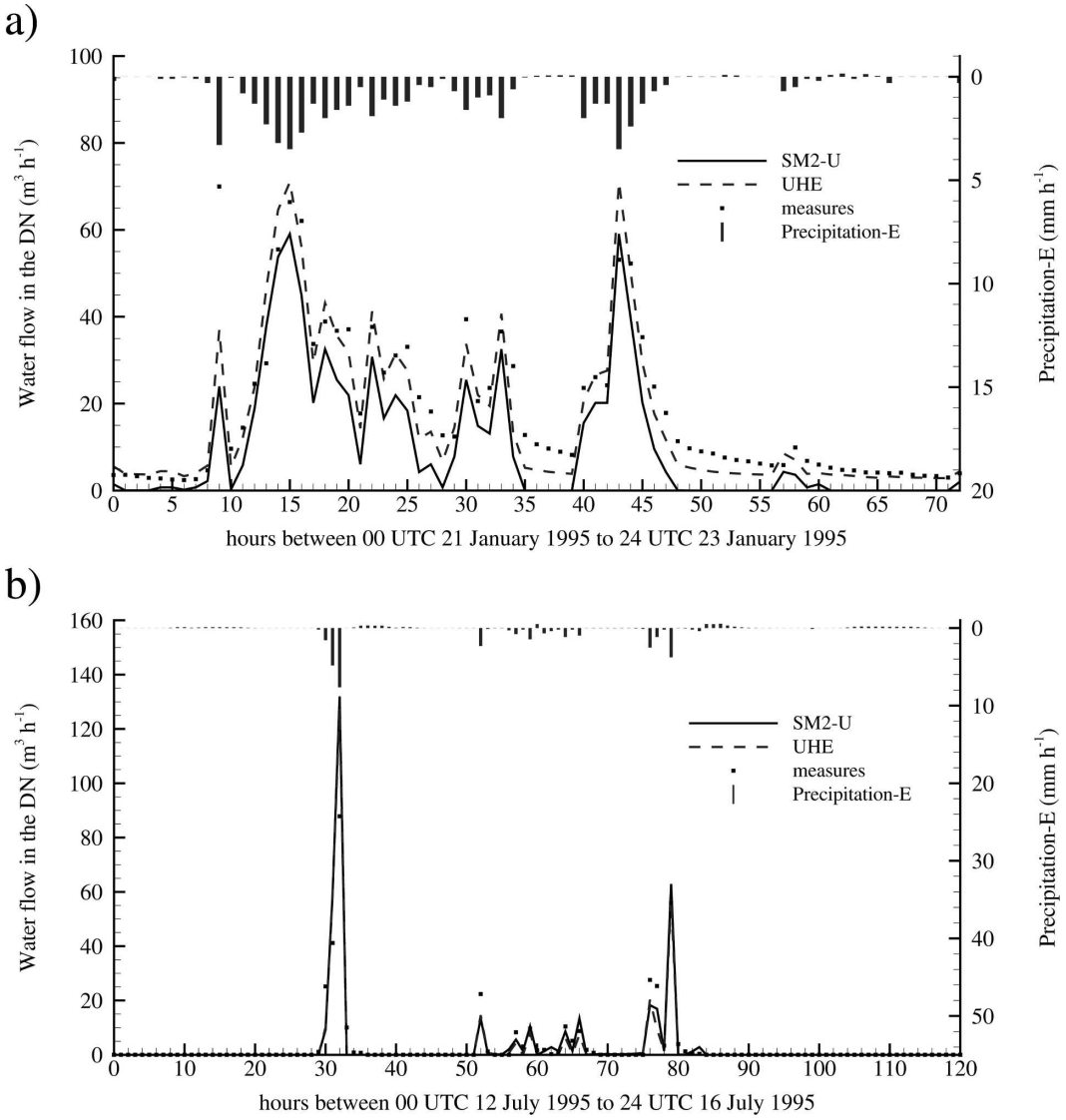

FIG. 9. Precipitation (minus evaporation) and water flow in the drainage network of the Rezé site during the two stormy events: (a) 21–23 Jan 1995 and (b) 12–16 Jul 1995 for the measurements at the drainage network outlet (dots), the SM2-U simulation (solid line), and the UHE simulation (dashed line).

tions. For the same period, the simulations with UHE are moderately better (Table 3).

Figure 8 separates the different water fluxes, normalized by the total precipitation; results regarding the SM2-U* version of the model are discussed in the next subsection. SM2-U and UHE are forced by the same observed precipitation, but the nighttime condensation is computed by SM2-U, yielding an additional 3.5% contribution. Water flows out of the domain three ways: from evapotranspiration, runoff toward the DN, and diffusion/drainage in the deep soil. On the average over the period, practically 100% of the water input leaves the domain because the gross water quantity inside the catchment is approximately the same at the beginning of 1994 and at the end of 1998. The evapotranspiration calculations of the two models are compared elsewhere (Berthier et al. 2006). SM2-U simulation yields 23% of the precipitation flows in the DN, while the evaluation with UHE is nearly 2 times larger, at 41%. Actually, the DN water flow evaluated by UHE adds up two processes: the direct runoff from the connected roofs, pavements, and natural surfaces, which account for 22.0%, and the infiltration of the soil water through the DN, which accounts for 19%, while SM2-U computes only the water runoff of the connected urban surfaces (roofs and pavements). The

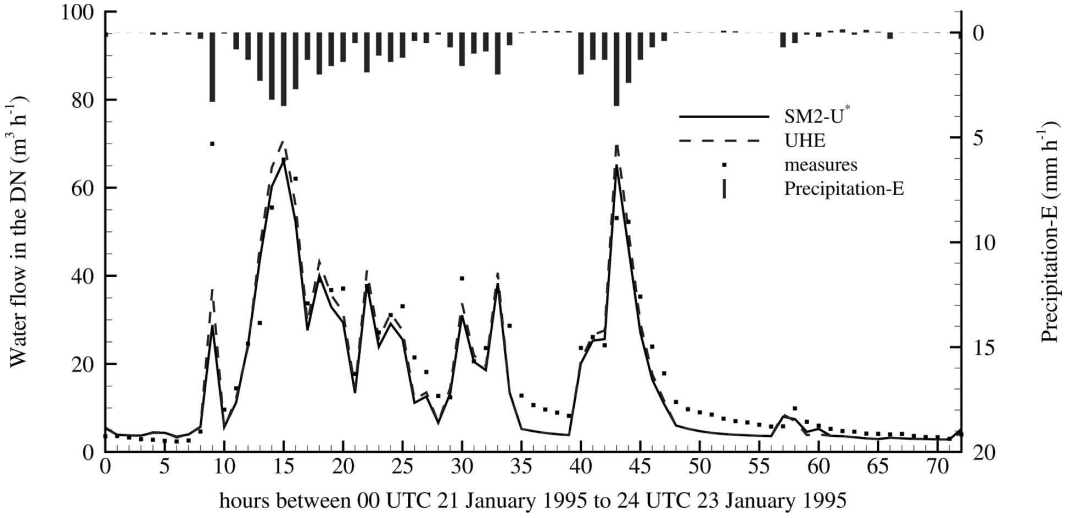

FIG. 10. Precipitation (minus evaporation) and water flow in the drainage network of the Rezé site during the stormy event of 21–23 Jan 1995 for the measurements at the drainage network outlet (dots), the SM2-U simulation with additional soil water infiltration forcing (solid line, SM2-U*), and the UHE simulation (dashed line).

amount of water streaming over the surfaces directly to the DN is approximately the same for the two models, which was rather expected because their roof and paved surface hydrological parameterizations are the same, and the bare soil runoff is very small here (0.7% according to the UHE evaluation). Thus, SM2-U underestimation of the DN water flow may be attributed to the lack of soil water infiltration calculation.

In Fig. 9, the DN water flow is observed in detail during two stormy events—one in winter (21–23 January 1995) and one in summer (12–16 July 1995). The winter storm is characterized by frequent precipitation during 40 h with a maximum intensity of 4 mm h^{-1}, whereas the summer storm is characterized by short and intense rains with a maximum intensity of 8 mm h^{-1} (1 mm $h^{-1} \equiv 1$ kg m^{-2} $h^{-1} = 3600^{-1}$ kg m^{-2} s^{-1}). The general behaviors of the simulations with SM2-U and UHE well match the measurements, which is expected because the outflow is directly driven by the precipitation inflow.

For the winter stormy period, the SM2-U flow is always lower than the observations. It increases very rapidly at the start of the rain, like measurements, but it also drops down to zero rapidly at the end of the rain periods, whereas the observed flows decrease extremely slowly, indicating that a large amount of water is provisionally stored during the rain and released afterward. As previously noted, with SM2-U the DN water flow includes only the runoff of (semi) impervious surfaces, when the water reservoirs overflow. When rain stops, the reservoirs stop overflowing and the model yields a null DN flow. In reality, when the rain stops the flow in the DN during the following hours comes from the soil water infiltration generated by the soil saturation during this winter period. This is well documented by UHE simulation; because UHE computes this infiltration rate, its DN water flow is always closer to that of the observations, especially after the rain stops.

For the summer period, the differences between the observed and simulated DN flows are quite small. With the soil being drier than during the winter and the rains being short and intense, the infiltration in the DN is negligible and the measured DN flow does correspond to the water runoff from the connected roofs and paved surfaces.

2) INFLUENCE OF WATER INFILTRATION FROM THE SOIL TO THE DRAINAGE NETWORK

The reference simulation demonstrated that soil water infiltration through DN pipes might be important contributions to the DN flow, especially for the evaluation at the scale of a storm and when the soil is saturated. But, as it concerns SM2-U (and ISBA), does this influence the surface latent heat flux evaluation, which is the key output of the hydrological model component?

To answer this question, in a second simulation SM2-U is forced both by the rain and by the infiltration process; a water quantity is removed from the root zone layer at each time step and added to the DN water flow. This modified simulation is referenced hereinafter as SM2-U*. Because measurements of the water infiltration are not available continuously, and because UHE

has been developed and validated with a special focus on this flow, the water quantity artificially transferred from the soil to the DN is here equal to the infiltration computed by UHE.

This SM2-U* simulation over the 5 yr appears largely improved (Table 3): the Nash criterion improves slightly, while the volume criterion is much better and positive (+1.9%), indicating a very small overestimation. The SM2-U* DN flow is now very close to that of the UHE simulation (Fig. 8). However, this model forcing hardly influences the evapotranspiration flux, which is 33.0% versus 32.8% in the reference simulation, and the DN flow increase of +22.1% is exactly compensated by the deep soil drainage decrease of −22.0%.

For the winter storm (Fig. 10) during which the influence of the soil water infiltration to the DN is important, the SM2-U* flow is now very close to the measurements, even between the rain periods.

It seems clear that modeling the soil water infiltration to the DN is required to evaluate correctly the DN flow, particularly when the soil is saturated. Yet, this does not seem to influence SM2-U surface flux evaluations because the amount of water of the root zone layer, which is eventually transmitted to the DN in reality, is anyway evacuated outside of the domain by the drainage of the root zone and deep soil layers in an adaptation of the soil processes to the atmospheric processes.

3) Model sensitivity to artificial surface parameters

In SM2-U water budget computation most parameters are either maintained from the ISBA original model or are well documented in handbooks. Yet, three parameters of the artificial surfaces are open to criticism: the maximum water storage capacity of the roofs $h_{\text{max roof}}$ and paved surfaces $h_{\text{max pav}}$, and the water infiltration capacity of the paved surfaces K_{pav}.

The values of the storage capacities seem difficult to assess and are highly variable with the state and shape of the surfaces and with the rain intensity (Hollis and Ovenden 1988a,b; Boyd et al. 1994), because they strongly depend on the surface type. As it concerns the infiltration capacity, the hydrological behavior of road coatings seems to largely differ when they are in place and are aging and cracked, from the laboratory observations. The effective values of K_{pav} may thus be disputable (see Berthier 1999; Ramier et al. 2004).

New simulations have been carried out, similar to the reference simulation but using different values of $h_{\text{max roof}}$, $h_{\text{max pav}}$, and K_{pav}.

Figure 11 represents, for the entire 1994–98 period, the partition of the water fluxes in the different surface types for the reference simulation and the two new sets

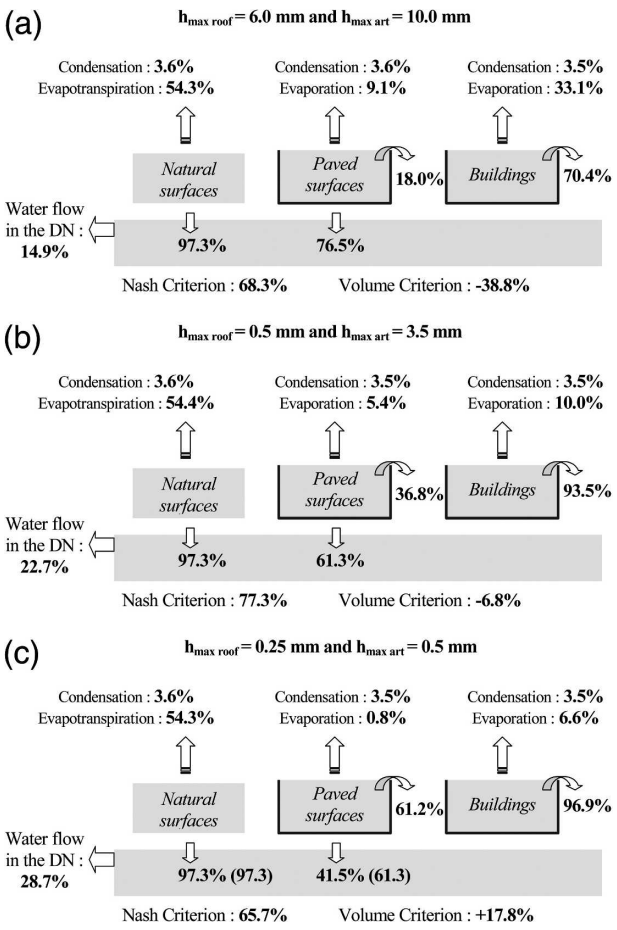

FIG. 11. Sensitivity of the water budgets of the SM2-U surface types at the Rezé site (natural surfaces, paved surfaces, and buildings) for the period of 1994–98, with respect to the maximum storage capacity of the urban reservoirs: $h_{\text{max roof}}$ and $h_{\text{max pav}}$. The water fluxes are in percent of the precipitation contribution to each surface type.

of $h_{\text{max } i}$ values, which crudely correspond to the extremes of the h_{max} ranges. When the reservoir storage capacities increase, the evaporation rates increase as well as the infiltration at the detriment of the runoff, thus decreasing the DN flow. The paved surface storage capacity influences the water infiltration in the soil, and therefore the root-zone-layer water content; yet, this does not appear to significantly modify the water budget of the natural surfaces (note that individual surface-type budgets do not seem balanced on this figure, e.g., natural surface losses largely exceed precipitation contribution, resulting from run-off and exchanges through the soil layer). The variations of water infiltration through the paved surfaces are not sufficient here to influence the vegetation transpiration (at least at the yearly scale).

The DN flow Nash and volume criteria of the new

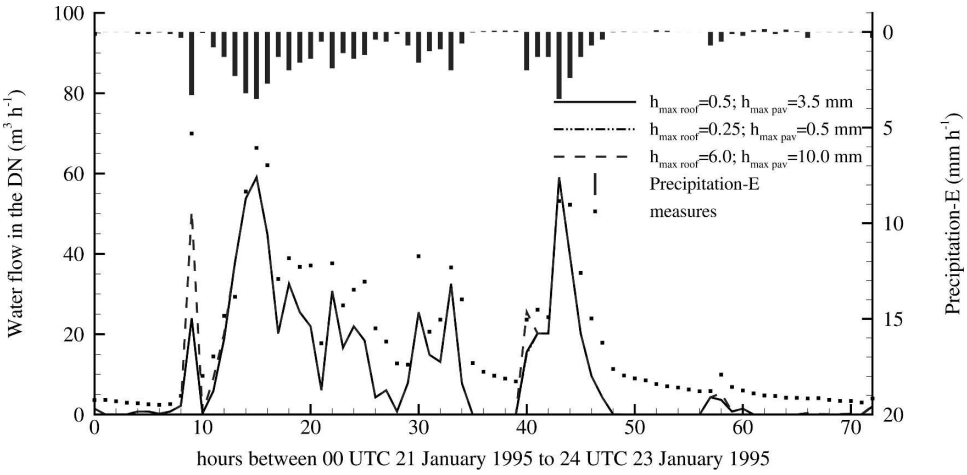

FIG. 12. Precipitation (minus evaporation) and water flow in the drainage network of the Rezé site during the stormy event of 21–23 Jan 1995 for the measurements at the drainage network outlet (dots), and the SM2-U simulations without additional soil water infiltration forcing with different values of $h_{\max\ roof}$ and $h_{\max\ pav}$ (lines).

simulations over the period of 1994–98 are largely worse than those of the reference simulation; the volume criterion is positive for the lower storage capacities, showing a large bias. Indeed, the reduction of the storage capacity of the reservoirs increases the surface runoff, which in turn minimizes the impact of the absence of soil water infiltration to the DN.

A focus on the January 1995 stormy period (Fig. 12) reveals marginal differences in the DN flow simulation at the beginning of each rain period preceded by a relatively drier period without rain, when all of the reservoirs are empty. Once all of the reservoirs are full the water total discharge in the DN is the same, independent of the storage capacity values. The simulation of DN flow between the showers is not improved.

Figure 13 represents, for 1994–98, the partition of the water fluxes in the different surface types for values of the hydraulic conductivity ranging over two orders of magnitude around the reference simulation value. The K_{pav} value strongly influences the water budget of the paved surfaces, changing the infiltration and both the runoff and the evaporation because the reservoir takes more time to be emptied by evaporation than by infiltration. Through the soil water content, K_{pav} marginally influences the water budget of the natural surfaces, but not at all that of the buildings, which is not linked to the soil water content. When K_{pav} decreases, the paved surface reservoir is less often empty and it refills more rapidly when the rain starts. Thus, K_{pav} reduction results in a large and positive volume criterion, that is, +25% versus −35.7% for the largest K_{pav}. The Nash criteria are also worse than in the reference simulation.

Significant differences are observed in the DN-simulated flow during the winter storm (Fig. 14). A lower conductivity increases the runoff and accelerates the discharge to the DN when the rains starts, but later the water infiltration through the paved surface continues as long as the reservoir is not empty. A larger conductivity definitely reduces the runoff and DN flow.

Before closing this subsection it must be noted that similar runoff sensitivities to these three parameters have been observed with the UHE hydrological model (Berthier 1999).

4) WATER BUDGET INFLUENCE ON THE LOCAL CLIMATOLOGY

After validation of the model on the Rezé site measurements, new simulations of the energy budget in situations close to that of the reference may emphasize the influence of the local water budget on the local climatology (only local effects may be demonstrated when the model is run in the stand-alone mode). Figure 15a displays the mean surface temperature diurnal cycle during the month of July 1996 in the reference simulation presented in the first subsection. Four new simulations have been run with only slight differences in the inputs, and the resulting differences in the mean temperature cycle are shown in Fig. 15b. All four runs would have simulated the suburban site behavior if 1996 had been a dry year (precipitation rates divided by 1000) while the weather remained otherwise unchanged (the general climatology of the French Atlantic coast around Nantes is very mild). The soil dryness is shown to increase the daytime surface temperature, with the difference exceeding 1.5 K from 0900 to 1600 LST. Observation of the energy budget components (not

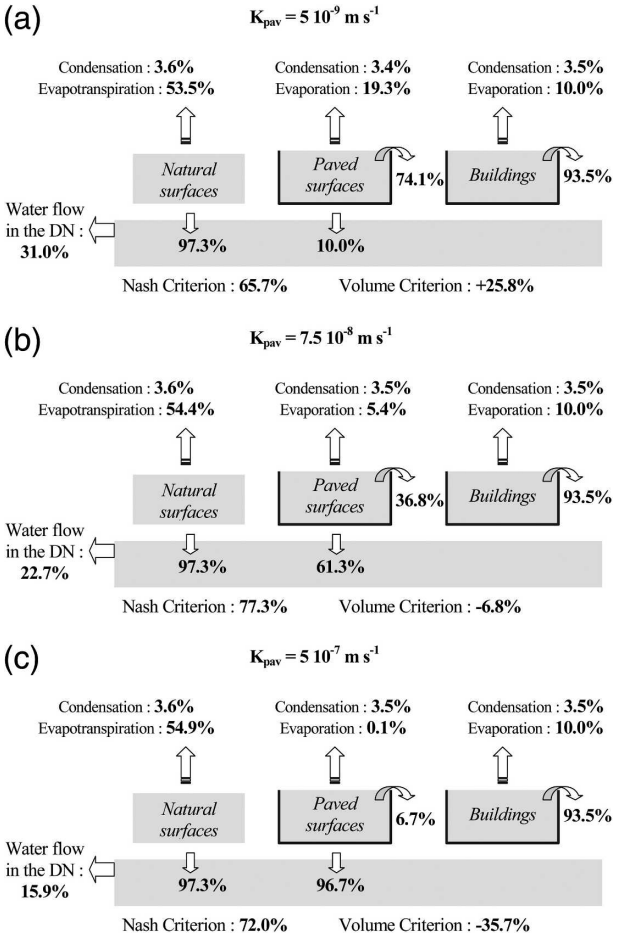

FIG. 13. Sensitivity of the water budgets of the SM2-U surface types at the Rezé site (natural surfaces, paved surfaces, and buildings) for the period of 1994–98, with respect to the hydraulic conductivity of the paved surface K_{pav}. The water fluxes are in percent of the precipitation contribution to each surface type.

shown) show that, in the reference simulation, the sensible and latent heat fluxes share equally about 85% of the net radiation (maximum 440 W m^{-2}), while the last 15% are stored in the ground during the daytime; at night the negative net radiation (about 40 W m^{-2}) is balanced by the storage heat release for 2/3 and by a small negative sensible heat flux for 1/3. The phase lag between the aerodynamic and storage flux cycles, typical of urban sites, is well observed, especially in the morning. With the dry soil, the latent heat flux drops to about 12% of the net radiation while the storage heat flux remains unchanged and the sensible heat flux balances some 73% of the budget. The second simulation includes vegetation watering: every day from 1900 to 2000 LST water is poured at a rate of 1 mm h^{-1} (1.45 kg m^{-2} s^{-1}) over the bare soil and 50% of the vegetation cover (figuring grass cover share). This moderate daily watering is shown to be sufficient for compensating for the soil dryness influence on the local climate; w_2 values (not shown) indicate that the upper soil layer remains close to saturation, and in this simulation the energy budget cycle appears very similar to that of the reference case. Consequently, the surface temperature is the same as in the reference case.

The last two simulations show the influence of realistic and antagonist layouts of the suburban settlement. In the case when the pavement of the road and parking lots is replaced by a stabilized grassy soil, which takes advantage of the evening watering to increase evapotranspiration, the mean temperature decreases 2° more all day long, and even 2.5 K at midday. On the contrary, the covering of vegetated surfaces by pavement strongly increases daytime surface temperatures, up to 5.5 K around 1200 LST (an increase from 24° to 30°C), without the effect of the evening watering because the soil water does not percolate upward through the pavement. In the last case the energy budget is largely perturbed because the heat storage is more than doubled, reaching 35% of the net radiation while the sensible heat flux reaches 93% of the net radiation, the budget being balanced by a large negative latent heat flux resulting from the downward flux of water vapor to the dry surface.

6. Summary and final remarks

SM2-U is a soil model developed for evaluating the heat fluxes at the urban canopy–atmosphere interface for atmospheric boundary layer models with high spatial resolution (hectometric scales). It has been developed as an urban extension of the ISBA force–restore model representing both rural and urban surfaces and any combination of natural and artificial cover modes that may be found in urban areas. The use of a force–restore equation for the prediction of the soil moisture content may be questioned because of the assumptions of periodic boundary forcing and of near-surface equilibrium between the capillarity and gravitational forces (Hu and Islam 1995). It is indisputable that a multilayer higher vertical resolution improves the accuracy of the numerical solution and vertical transfer of water, but it also increases largely the computational time. Indeed, force-restore models whose coefficients have been carefully calibrated against multilayer models have been shown to simulate rural areas with the same accuracy as these last ones (see, e.g., Boone et al. 1999; Shao and Henderson-Sellers 1996). Thus, for the urban applications of SM2-U the force-restore approach seems a good compromise between computational time demand and accuracy of the evapotranspiration.

While ISBA computes the energy budgets with a unique, composite surface temperature for the ground–

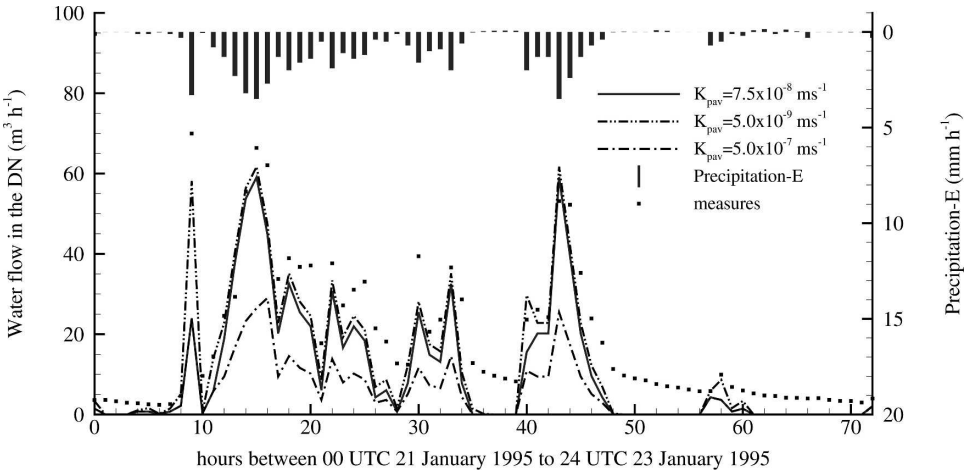

FIG. 14. Precipitation (minus evaporation) and water flow in the drainage network of the Rezé site during the stormy event of 21–23 Jan 1995 for the measurements at the drainage network outlet (dots) and the SM2-U simulations without additional soil water infiltration forcing with different values of K_{pav} (lines).

vegetation systems, the larger number of cover modes in urban areas requests that SM2-U evaluates separately their energy budgets with their own surface temperatures. The comparison of SM2U simulations of HAPEX-MOBILHY and EFEDA data with those of the original version validates this choice, showing that the separation does not alter the model performances. On the contrary, for these rural sites it tends to improve them while it mainly allows for much better control of the model strengths and weaknesses on physical arguments.

The model does not compute any ground horizontal transfers explicitly. Hence, fast transfers in the soil layers are implicitly assumed because soil temperature and water content are unique in a cell, redistributing the available soil heat and moisture. At very fine spatial resolution, less than a kilometer, there is little chance that a model grid mesh contains only purely rural vegetation and purely urban surfaces, impervious and fully connected to the drainage network, in equal shares. A high-resolution grid box containing a mixture of natural and impervious surfaces, with a large density of impervious ones connected to the drainage network, is likely to be an area where vegetation does suffer from the reduction of soil moisture because it is drained under the impervious surfaces. This is one of the reasons for a policy change in many European countries to encourage rainwater diversion from the impervious surfaces to the neighboring vegetated areas (rather than to the DN), especially in suburban areas. Yet, if the model is used with larger grid meshes, some vegetated areas neighboring large impervious surfaces (e.g., commercial centers) may have access to an incorrect amount of soil moisture because the model would implicitly assume long-distance water transfers in the soil. This should be checked and taken care of by, for example, disconnecting the soil layers under the two types of surfaces.

The model simulations of the suburban settlement of Rezé have been compared with the unique 5-yr urban catchment experimental dataset and to simulations with UHE, a hydrological model that had been previously validated. The water flow in the draining network is well simulated by SM2-U at the annual scale and during a summer stormy period, but it is underestimated during a winter storm period, especially between the rains, because SM2-U does not compute the water infiltration from the soil to the DN through the pipe system water tightness defects, which may be important when the soil is saturated.

To assess the influence of this flow on SM2-U evapotranspiration flux evaluation, the reference simulation has been repeated with an additional forcing, where the infiltration soil water (as calculated by UHE in parallel) was removed from the root zone layer at each time step and transferred to the DN flow. This forced simulation produced a better evaluation of the water flow in the DN during the winter storm event, showing that a parameterization of the soil water infiltration must be added to evaluate precisely the DN flow. This parameterization could be a function of the root-zone-layer water content, the surface of exchange between the DN and the soil, and the hydraulic conductivity of the DN pipes. On the contrary, this infiltration forcing has no influence on the simulated surface fluxes. Indeed, the amount of water in the root zone layer, which eventually percolates in the DN, is evacuated as well by the model drainages from the root zone and deep soil lay-

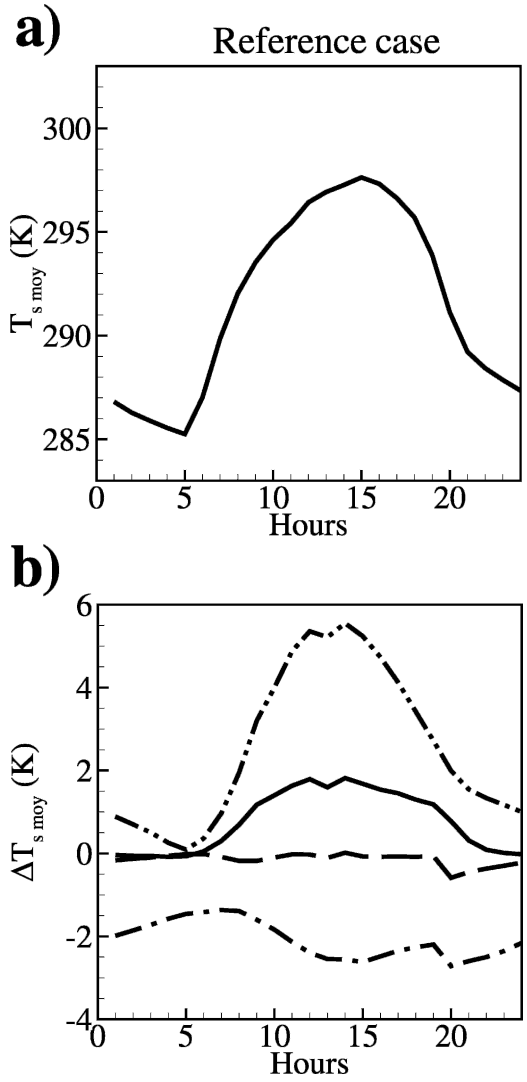

FIG. 15. Influence of surface layout on the Rezé suburban settlement mean surface temperature: (a) surface temperature diurnal cycle in the reference simulation averaged over the month of July 1996 and (b) difference with the reference simulation for a dry year with no layout change (solid line), vegetation evening watering (dash line), grassy ground for roads and parking lots (dash–dot line), and natural grounds covered with pavement (dash–dot–dot line).

ers, such that the water contents of the soil layers remain unchanged with or without the additional infiltration forcing. For the urban atmospheric boundary layer simulations, SM2-U does not need an additional parameterization of the infiltration process.

A sensitivity study has been launched with respect to some poorly assessed hydrological parameters of the artificial urban surfaces—the maximum water storage capacities of roofs and paved surfaces, and the paved surface hydraulic conductivity. The DN flow and the evaporation from urban surfaces are both largely influenced by these parameters. For the simulation of the urban boundary layer during and after showers and stormy events, the hydrological characteristics of semiimpervious surfaces appear to be of extreme importance because these parameters regulate the intensity of short-term evaporation in urban areas.

The prospective simulations presented in the last subsection show that the water budget modeling quality is utterly important for the evaluation of the local urban microclimatology, for instance, in alternative layout scenarios in areas where vegetated and artificial surfaces are intermixed, which represent the largest fraction of the European urban areas.

As a physically based model, SM2-U requires input parameters describing the canopy morphology and physical properties as well as the ground texture. The development of such models is supported for the last few years by the increase of the computer performances and the geographical information system (GIS) and spatial dataset availability. Hence, for atmospheric model inputs detailed urban morphology datasets have been constructed from land use/land cover databases and/or from airborne lidar measurements with a horizontal and vertical accuracy of a few centimeters, see, for example, Burian et al. (2004) and Dupont et al. (2004b) for the city of Houston, Texas, or Long et al. (2003) for the city of Marseille, France. However, some parameters of the model are still difficult to measure and need to be determined or calibrated from the model applications, such as the vegetation minimum stomatal resistance or the effective hydrological parameters of urban surfaces (semiimpervious materials and restructured soils). For these last parameters, the current knowledge remains insufficient, especially because it appears to be highly variable in time and dependent on rain intensity and duration (Hollis and Ovenden 1988a). Additional experimental assessments of such urban surfaces are needed.

Acknowledgments. This paper was partly written when the first author was with the U.S. EPA NERL/AMD/ASPMB, at Research Triangle Park, North Carolina. This work was funded by the CNRS national research program in hydrology (INSU/PNRH, Grant 02CV027).

REFERENCES

André, J.-C., J.-P. Goutorbe, and A. Perrier, 1986: HAPEX-MOBILHY: A hydrologic atmospheric experiment for the study of water budget and evaporation flux at the climatic scale. *Bull. Amer. Meteor. Soc.,* **67,** 138–144.

Belhadj, N., C. Joannis, and G. Raimbault, 1995: Modelling of

rainfall induced infiltration into separate sewerage. *Water Sci. Technol.,* **32,** 161–168.

Berthier, E., 1999: Contribution à une modélisation hydrologique à base physique en milieu urbain. Ph.D. thesis, INPG–LCPC, 196 pp.

——, F. Rodriguez, and H. Andrieu, 1999: The Rezé urban catchments database. *Water Resour. Res.,* **35,** 1915–1919.

——, H. Andrieu, and J. D. Creutin, 2004: The role of soil in the generation of urban runoff: Development and evaluation of a 2D model. *J. Hydrol.,* **299,** 252–266.

——, S. Dupont, P. G. Mestayer, and H. Andrieu, 2006: Comparison of two evapotranspiration schemes on a sub-urban site. *J. Hydrol.,* in press.

Best, M. J., 2005: Representing urban areas within operational numerical weather prediction models. *Bound.-Layer Meteor.,* **114,** 91–109.

Bolle, H. J., and Coauthors, 1993: EFEDA: European Field Experiment in a Desertification-threatened Area. *Ann. Geophys.,* **11,** 173–189.

Boone, A., J. C. Calvet, and J. Noilhan, 1999: Inclusion of a third soil layer in a land surface scheme using the force-restore method. *J. Appl. Meteor.,* **38,** 1611–1630.

Bottema, M., 1997: Urban roughness modelling in relation to pollutant dispersion. *Atmos. Environ.,* **31,** 3059–3075.

Boyd, M. J., M. C. Bufill, and R. M. Knee, 1994: Predicting pervious and impervious storm runoff from urban drainage basins. *Hydrol. Sci.,* **39,** 321–332.

Braud, I., J. Noilhan, J. Bessemoulin, and P. Mascart, 1993: Bare-ground surface heat and water exchanges under dry conditions: Observations and parameterization. *Bound.-Layer Meteor.,* **66,** 173–200.

Burian, S., S. Stetson, W. Han, J. K. S. Ching, and D. Byun, 2004: High resolution dataset of urban canopy parameters for Houston, Texas. Preprints, *Fifth Urban Environment Symp.*, Vancouver BC, Canada, Amer. Meteor. Soc., CD-ROM, 9.3.

Clapp, R., and G. Hornberger, 1978: Empirical equations for some soil hydraulic properties. *Water Resour. Res.,* **14,** 601–604.

Danish Hydraulic Institute, 1996: An integrated modelling package for urban drainage and sewer systems. MOUSE user manual, CD-ROM, version 4.0.

Deardorff, J. W., 1978: Efficient prediction of ground surface temperature and moisture with inclusion of a layer of vegetation. *J. Geophys. Res.,* **83,** 1889–1903.

Dupont, S., 2001: Modélisation dynamique et thermodynamique de la canopée urbaine: Réalisation du modèle de sols urbains pour SUBMESO. Ph.D. thesis, Université de Nantes, 319 pp.

——, and P. G. Mestayer, 2004: Evaluation of the urban soil model SM2-U on the city center of Marseille (France). Preprints, *Fifth Symp. on Urban Environment*, Vancouver, BC, Canada, Amer. Meteor. Soc., CD-ROM, 9.14.

——, and ——, 2006: Parameterization of the urban energy budget with the Submesoscale Soil Model. *J. Appl. Meteor. Climatol.,* in press.

——, I. Calmet, and P. G. Mestayer, 2002: Urban canopy modeling influence on urban boundary layer simulation. Preprints, *Fourth Symp. on Urban Environment*, Norfolk, VA, Amer. Meteor. Soc., 151–152.

——, T. L. Otte, and J. K. S. Ching, 2004a: Simulation of meteorological fields within and above urban and rural canopies with a Mesoscale Model (MM5). *Bound.-Layer Meteor.,* **113,** 111–158.

——, J. K. S. Ching, and S. Burian, 2004b: Introduction of urban canopy parameterizations into MM5 to simulate meteorology at neighborhood scales. Preprints, *Symp. on Planning, Nowcasting, and Forecasting in the Urban Zone*, Seattle, WA, Amer. Meteor. Soc., CD-ROM, 4.4.

Giordani, H., J. Noilhan, P. Lacarrere, P. Bessemoulin, and P. Mascart, 1996: Modelling the surface processes and the atmospheric boundary layer for semi-arid conditions. *Agric. For. Meteor.,* **80,** 263–287.

Goutorbe, J. P., 1991: A critical assessment of the SAMER network accuracy. *Land Surface Evaporation: Measurement and Parameterization*, T. J. Schmugge and J. C. André, Eds., Springer-Verlag, 171–182.

Grimmond, C. S. B., and T. R. Oke, 1991: An evapotranspiration-interception model for urban areas. *Water Resour. Res.,* **27,** 1739–1755.

——, and ——, 1999: Heat storage in urban areas: Local-scale observations and evaluation of a simple model. *J. Appl. Meteor.,* **38,** 922–940.

——, and ——, 2002: Turbulent heat fluxes in urban areas: Observations and a Local-Scale Urban Meteorological Parameterization Scheme (LUMPS). *J. Appl. Meteor.,* **41,** 792–810.

——, T. S. King, M. Roth, and T. R. Oke, 1998: Aerodynamic roughness of urban areas derived from wind observations. *Bound.-Layer Meteor.,* **89,** 1–24.

Guilbaud, C., 1996: Etude des inversions thermiques: Application aux écoulements atmosphériques dans des vallées encaissées. Ph.D. thesis, University Joseph Fourier, 189 pp.

Guilloteau, E., 1998: Optimized computation of transfer coefficients in surface layer with different momentum and heat roughness lengths. *Bound.-Layer Meteor.,* **87,** 147–160.

——, 1999: Modélisation des sols urbains pour les simulations de l'atmosphère aux échelles sub-meso. Ph.D. thesis, Ecole Centrale and University of Nantes, 160 pp.

Hollis, G. E., and J. C. Ovenden, 1988a: The quantity of stormwater runoff from ten stretches of road, a car park and eight roofs in Hertfordshire, England during 1983. *Hydrol. Processes,* **2,** 227–243.

——, and ——, 1988b: One year irrigation experiment to assess losses and runoff volume relationships for residential road in Hertfordshire, England. *Hydrol. Processes,* **2,** 61–74.

Hu, Z., and S. Islam, 1995: Prediction of ground surface temperature and soil moisture content by the force–restore method. *Water Resour. Res.,* **31,** 2531–2539.

INSAVALOR and Sogreah, 1997: CANOE, logiciel d'hydrologie urbaine, conception et évaluation de réseaux d'assainissement, simulation des pluies, des écoulements et de la qualité des eaux. Users manual, 476 pp.

Jacquemin, B., and J. Noilhan, 1990: Sensitivity study and validation of a land surface parameterization using the HAPEX-MOBILHY data set. *Bound.-Layer Meteor.,* **52,** 93–134.

Jia, Y., G. Ni, Y. Kawahara, and T. Suetsugi, 2001: Development of WEP model and its application to an urban watershed. *Hydrol. Processes,* **15,** 2175–2194.

Lemonsu, A., and V. Masson, 2002: Simulation of a summer urban breeze over Paris. *Bound.-Layer Meteor.,* **104,** 463–490.

Long, N., G. Pigeon, P. G. Mestayer, P. Durand, and C. Kergomard, 2003: Correlation between temperature and classification of urban fabric on Marseille during ESCOMPTE. *Proc. Fifth Int. Conf. on Urban Climate,* Lodz, Poland, 95–98.

Mahura, A., P. G. Mestayer, S. Dupont, I. Calmet, A. Baklanov, S. Leroyer, and N. Long, 2004: Comparison of short and long-term modelled latent, sensible, and storage heat fluxes employing numerical weather prediction model with and

without urbanized modules. *Proc. Fourth Annual Meeting of the European Meteorological Society*, Vol. 1, Nice, France, European Meteorological Society, 391.

Martilli, A., A. Clappier, and M. W. Rotach, 2002: An urban surface exchange parameterization for mesoscale models. *Bound.-Layer Meteor.,* **104,** 261–304.

Masson, V., 2000: A physically-based scheme for the urban energy budget in atmospheric models. *Bound.-Layer Meteor.,* **98,** 357–397.

Monteith, J. L., 1976: *Case Studies*. Vol. 2, *Vegetation and the Atmosphere*, Academic Press, 439 pp.

Nash, J. E., and J. V. Sutcliffe, 1970: River flow forcasting through conceptual models. Part I—A discussion of principle. *J. Hydrol.,* **10,** 282–290.

Noilhan, J., and S. Planton, 1989: A simple parameterization of land surface processes for meteorological models. *Mon. Wea. Rev.,* **117,** 536–549.

——, and J.-F. Mahfouf, 1996: The ISBA land surface parameterisation scheme. *Global Planet. Change,* **13,** 145–159.

Pleim, J. E., and A. Xiu, 1995: Development and testing of a surface flux and planetary boundary layer model for application in mesoscale models. *J. Appl. Meteor.,* **34,** 16–32.

Raimbault, G., 1996: Effet des sols et sous-sol urbains sur le devenir des eaux pluviales. *Bull. Lab. Ponts Chaussées,* **202,** 71–78.

Ramier, D., E. Berthier, and H. Andrieu, 2004: An urban lysimeter to assess runoff losses on asphalt concrete plates. *Phys. Chem. Earth,* **29,** 839–847.

Raupach, M. R., 1992: Drag and drag partition on roughness surfaces. *Bound.-Layer Meteor.,* **60,** 375–395.

Rossman, L. A., 2004: Storm Water Management Model. User's manual version 5.0, United States Environmental Protection Agency, 235 pp.

Shao, Y., and A. Henderson-Sellers, 1996: Validation of soil moisture simulation in land surface parameterization schemes with HAPEX data. *Global Planet. Change,* **13,** 11–46.

Wallingford Software, Ltd., cited 1997: Using HydroWorks. [Available online at http://www.wallingfordsoftware.com/.]